frontiers | Frontiers in Environmental Science

TYPE Original Research
PUBLISHED 11 July 2024
DOI 10.3389/fenvs.2024.1369678

OPEN ACCESS

EDITED BY
Mounia Tahri,
National Centre for Nuclear Energy, Science and Technology, Morocco

REVIEWED BY
Mauro Masiol,
Ca' Foscari University of Venice, Italy
Solomon Giwa,
Olabisi Onabanjo University, Nigeria

*CORRESPONDENCE
Stefania Renna,
stefania.renna@cmcc.it

RECEIVED 12 January 2024
ACCEPTED 06 June 2024
PUBLISHED 11 July 2024

CITATION
Renna S, Lunghi J, Granella F, Malpede M and Di Simine D (2024), Impacts of agriculture on PM_{10} pollution and human health in the Lombardy region in Italy.
Front. Environ. Sci. 12:1369678.
doi: 10.3389/fenvs.2024.1369678

Impacts of agriculture on PM_{10} pollution and human health in the Lombardy region in Italy

Stefania Renna[1,2,3]*, Jacopo Lunghi[1,2,4], Francesco Granella[1,2,4], Maurizio Malpede[5] and Damiano Di Simine[6]

[1]CMCC Foundation—Euro-Mediterranean Center on Climate Change, Lecce, Italy, [2]RFF-CMCC European Institute on Economics and the Environment, Milan, Italy, [3]Department of Management, Economics and Industrial Engineering, Politecnico di Milano, Milan, Italy, [4]Department of Social and Political Sciences, Bocconi University, Milan, Italy, [5]Department of Economics, University of Verona, Verona, Italy, [6]Legambiente, Rome, Italy

Air pollution is one of the main environmental health concerns globally, with particulate matter (PM) as the primary threat. While many policies address emissions from transport and industry, there is growing evidence of agriculture's significant impact on air quality. Evaluating how intensive farming impacts PM concentrations and public health is necessary for informed policy interventions. We focus on the Po Valley (Italy), characterized by intensive agricultural practices and substantial pollution levels. Our study examines secondary inorganic aerosol (SIA) concentrations between 2013 and 2020 in Lombardy. Our findings reveal key insights into the impact of intensive farming on air pollution and public health. First, we find that ammonium salts make up over 30% of the daily particulate matter $\leq$ 10 μ m (PM_{10}), with annual levels [11.6–11.8 $\mu g/m^3$] reaching half of the European Union's proposed limit (20 $\mu g/m^3$). Second, exposure tends to peak in low-wind conditions. In Milan, ammonia predominantly flows from the east, aligning with heavy livestock activity, while nitrogen oxides' (NO_x) impacts seem more localized. Rural SIA peaks correlate with winds from NO_x-rich areas. These outcomes imply that targeted, single-sector policies might fall short of significantly reducing PM_{10} concentrations. Additionally, manure spreading raises SIA levels by 2–3 $\mu g/m^3$ in urban backgrounds the following days. Local sources also stand out in back-trajectory modeling of concentrations. Finally, applying long-term concentration-response functions to ammonium salts as a fraction of PM_{10}, our study suggests that pollution stemming from agricultural activities in Milan leads to approximately 589 [446–866] deaths annually, resulting in an average loss of 6,951 [5,267–10,222] life years. This equates to 43 [33–64] deaths and 511 [387–751] lost life years for every 100,000 residents.

KEYWORDS

coarse particulate matter (PM10), secondary inorganic aerosol (SIA), ammonium salts, agriculture, back-trajectories, human health, attributable deaths (AD), years of life lost (YLL)

1 Introduction

The European Environment Agency (EEA) and the World Health Organization (WHO) rank air pollution as Europe's greatest environmental health risk. Outdoor air pollution alone is responsible for more than 327,000 premature deaths every year. Fine particulate matter with a diameter less than or equal to 2.5 μm ($PM_{2.5}$) is shown to be the most harmful pollutant, with 253,000 premature deaths attributable to exposure above 5 micrograms per cubic meter of air ($\mu g/m^3$) among the European Union (EU) member states, 46,800 of which being attributed to Italy alone (European Environment Agency, 2023b).

In Italy, the majority of fatalities occur in the Po Valley, a densely populated and highly industrialized region of Northern Italy with some of the highest particulate matter (PM) concentrations among OECD countries (European Environment Agency, 2023a). Due to this basin's unique geo-morphological and meteorological conditions, the chemical regimes of PM are complex, non-linear, and spatially varying, exacerbating pollution levels (Thunis et al., 2021).

Additionally, the Po Valley is a hub for intensive agricultural activities and livestock farming, resulting in high atmospheric ammonia (NH_3) (Carozzi et al., 2012; Damme et al., 2014; Van Damme et al., 2018). Almost all of the regional NH_3 emissions are attributed to agriculture (INEMAR - ARPA Lombardia, 2022). Agriculture plays a critical role in producing harmful secondary PM (Cambra-López et al., 2010; Lelieveld et al., 2015; Lovarelli et al., 2020; McDuffie et al., 2021; Belis et al., 2021). According to Lelieveld et al. (2015), the agricultural sector is responsible for the highest incidence of premature mortality caused by air pollution in Europe: in Italy, approximately 39% of premature deaths due to $PM_{2.5}$ and tropospheric ozone (O_3) can be attributed to agriculture. As several studies suggest, curbing secondary PM precursor emissions, such as NH_3 and nitrogen oxides (NO_x), may decrease PM levels (Clappier et al., 2021; Veratti et al., 2023), and reduce premature deaths due to PM exposure (Lelieveld et al., 2015; Lee et al., 2015; Pozzer et al., 2017; Giannadaki et al., 2018; Thakrar et al., 2020; Wyer et al., 2022), providing relevant economic benefits (Giannadaki et al., 2018). However, NH_3 is the pollutant with the lowest decline in emissions (−12.1%) in Europe over 2005–2021, trailing by a large margin $PM_{2.5}$ (almost one-third in reduction), NO_x (almost half), and SO_2 (four-fifths) (European Environment Agency, 2023c).

Concerning both short and long-term PM components' toxicity and their related effects on health, the existing research is still insufficient (Kinney et al., 2010; Atkinson et al., 2014; Chung et al., 2015; Wyzga and Rohr, 2015; Badaloni et al., 2017; Chen and Hoek, 2020), in particular on the role of nitrates and sulfates (Cassee et al., 2013; World Health Organization Regional Office for Europe, 2013). Some studies suggest that the inorganic components of PM might be less detrimental than the carbonaceous part (Schlesinger and Cassee, 2003), which could be up to five times more harmful (Tuomisto et al., 2008; Lelieveld et al., 2015), and than combustion aerosols in general (Park et al., 2018). However, other researchers have obtained different findings. Achilleos et al. (2017) find in their meta-analysis that the short-term association between $PM_{2.5}$ and cardiovascular mortality weighs the same for elemental carbon and nitrate, while the former has a stronger association for total mortality. In a Chinese province, nitrate, ammonium, and organic matter have been observed to affect mortality more strongly relative to other $PM_{2.5}$ components, as reported by Fu et al. (2023).

Numerous analyses on the role of agriculture on air pollution and on the spatiotemporal distribution of NH_3 levels in Lombardy have been conducted (Lonati and Cernuschi, 2020; Lovarelli et al., 2021; Belis et al., 2021; Thunis et al., 2021; Veratti et al., 2023; Fassò et al., 2023; Lunghi et al., 2024; Granella et al., 2024; Otto et al., 2024; Pietrogrande et al., 2022; Colombo et al., 2024), as well as on secondary inorganic aerosol (SIA) formation (Andreani-Aksoyoglu et al., 2004; Lonati et al., 2008; Bedogni and Pirovano, 2011; Daher et al., 2012; Pirovano et al., 2015; Perrone et al., 2016; Pietrogrande et al., 2022; Granella et al., 2024; Amato et al., 2024). We build on a recent study by Lonati and Cernuschi (2020), that analyzes spatial and temporal patterns characterizing NH_3 concentrations in Lombardy and their influence on urban areas. Our work adds to the literature by providing an extensive analysis of SIA patterns using the most recent and novel data. We use correlational analyses to explore the contribution of agriculture to PM_{10} formation and its human health impacts in Lombardy, the most populous region in Italy.

Given that the most critical health impacts originate from PM itself, unlike previous studies, we focus on SIA, a component of PM, rather than NH_3, a precursor. We analyze the inorganic component of PM, ammonium salts, i.e., the sum of ammonium nitrate (NH_4NO_3) and ammonium sulfate ($(NH_4)_2SO_4$) in PM_{10}, derived from three air quality stations located in the region. By examining the contribution of ammonium salts to the total PM_{10} mass, we gain valuable insights into the potential sources of the inorganic component. We also investigate the extent to which ammonium salts alone contribute to the exceeding of both EU-prescribed limits and WHO-recommended levels, thereby clarifying the importance of SIA mitigation policies to achieve the normative limits and minimize their health impacts. We then use polar plots and back-trajectory modeling to determine local and distant source contribution and spatial correlation at receptor sites.

Our study is one of the few exploring long-range transport patterns and their impact on SIA formation in Lombardy across a long time series. One of the agricultural activities with a substantial impact on SIA formation is the broadcasting of manure. We look at the impact of manure spreading on the observed SIA levels in Milan. Finally, we evaluate the health impact of agriculture. This involves estimating the number of deaths and years of life lost attributable to exposure to ammonium salts as a fraction of PM_{10} by using concentration-response functions for PM_{10} available in existing literature. Additionally, we compute these impacts by both gender and quinquennial age groups. To the best of our knowledge, no prior study directly associates the levels of ammonium salts in PM_{10} with a long-term health burden in Lombardy.

2 Materials and methods

2.1 Data

2.1.1 PM and secondary inorganic aerosol

PM may either be directly emitted into the atmosphere through biogenic or anthropogenic emissions (primary aerosol) or may indirectly result from chemical reaction processes (secondary aerosol) (Seinfeld and Pandis, 2016). In Europe's urban

environments, including the Po Valley, the secondary aerosol component of PM prevails in the total mass concentration (Larsen et al., 2012; Aksoyoglu et al., 2017; Thunis et al., 2021; Clappier et al., 2021).

Depending on the composition, secondary aerosol may be classified as secondary organic aerosol (SOA) or as secondary inorganic aerosol (SIA). Gaseous precursors of the SIA are atmospheric NH_3, NO_x, and SO_2, which react in the atmosphere to form NH_4NO_3 $(NH_4)_2SO_4$, and ammonium bisulfate (NH_4HSO_4), also known as ammonium salts due to the presence of the ammonium cation (NH_4^+) (Larsen et al., 2012; Squizzato et al., 2013; Lonati and Cernuschi, 2020). The first two are NH_4NO_3's precursors, while the first and the latter are precursors of $(NH_4)_2SO_4$, and therefore contribute to PM_{10}. While NH_3 has an expected lifetime of roughly 10 days due to its high solubility in the ground and in waters (Seinfeld, 2016), ammonium salts such as NH_4NO_3 may last longer, up to about 2 weeks, being prone to long-range transport (Ehrnsperger and Klemm, 2021).

In Italy, NO_x emissions come mainly from traffic, industry, and the power sector, while SO_2 is emitted by the industrial and power sectors. NH_3 emissions, however, come almost entirely from the agricultural sector, and predominantly from livestock farming and manure management (as much as 97.1% and 86.5%, respectively, in Lombardy) (INEMAR - ARPA Lombardia, 2022).

2.1.2 Study area

Lombardy, located in Northern Italy within the Po Valley, is the region with the highest number of livestock units and intensive rearing in the country. It also stands among the leading regions in Europe in terms of livestock (Statistical Office of the European Union, 2023). Refer to Supplementary Figure S1 to compare cattle and pig livestock numbers in Lombardy with other European regions. As of the conclusion of 2021, Lombardy housed approximately 27.58% of the Italian cattle population, amounting to 1,555,372 units, and a substantial 50.55% of the Italian pig population, totaling 4,242,918 units (Pretolani and Rama, 2022). Notably, within the category of ruminants with significant dietary requirements, more than one-fourth of milk cows were found in Lombardy. However, Lombardy's breeding farms represented only 10% and 8.84% of the Italian total for cattle and pigs, respectively. In the context of agricultural emissions of NH_3, while crops contribute 7%, livestock effluent management accounts for 93%, of which bovine and swine farming alone constitute 52.5% and 27.1%, respectively. The remaining 13.5% of emissions are attributed to the farming of other animals.

Due to its high anthropogenic activity but also to its geographical characteristics, Lombardy is particularly subject to the accumulation of pollutants and poor air quality for prolonged periods. In particular, the presence of the Alps on the northern and western side and of the Apennines on the southern side determine weak wind conditions and frequent thermal inversion episodes, hindering atmospheric dispersion and trapping pollution to the ground (Caserini et al., 2017).

2.1.3 Data sources

In this study, we employed a wide range of data types, including air quality, meteorological conditions, livestock, crop areas, effluent dispersion, population demographics, and mortality statistics. All of these data sets are readily accessible online, with the exception of PM speciation data, which are provided by the regional environmental protection agency, *Agenzia Regionale per la Protezione dell'Ambiente* (ARPA Lombardia), which is in charge of collecting samples and validating the data for the territory of Lombardy in the appliance of the European Directive on Air Quality (European Union, 2008). For further details on the analytical methods followed by ARPA Lombardia and the instrumentation employed, see Supplementary Section S1. Supplementary Tables S1, S2 report the limit of detection and the uncertainty associated with the ions' measurements.

Specifically, we have gathered daily data on air pollutants from the Open Data Lombardia portal (Regione Lombardia, 2021), with a particular focus on select pollutants and trace gases, including PM_{10}, NO_x, and NH_3. Our research is primarily focused on daily PM_{10} speciation data, which have been subject to post-processing to derive ammonium salts. Note that the method employed to estimate NH_4NO_3 and $(NH_4)_2SO_4$ concentrations relies on the assumption of pure salts, a simplification that could impact the accuracy of our estimations. On the one hand, the interactions between nitrate, sulfate, and substances different from NH_4^+ (e.g., sea salt, sodium, calcium, chlorine, potassium) could lead to the formation of mixed salts (Seinfeld, 2016). For example, if nitrate reacts with sea salt to form sodium nitrate, the actual amount of NH_4NO_3 would be less than what is estimated under the assumption of pure salts. On the other hand, the available NH_4^+ may be consumed with other acids, e.g., hydrochloric acid to form ammonium chloride. Such cases would both imply an overestimation of NH_4NO_3 and $(NH_4)_2SO_4$. In this matter, the availability of NH_3, which is abundant in the region, and other pollutants are crucial for forming these aerosols. Such concerns are partly reduced by the fact that NH_4^+ is the most prevalent ion compared to the others (see Supplementary Tables S3–S5). For a more comprehensive understanding of the formation of SIA and the calculation of ammonium salts, additional information can be found in Supplementary Section S2, S3.

Concentrations are expressed in $\mu g/m^3$. The data set covers the period from 2013 to 2020 and has been collected from three air quality monitoring stations located within the Lombardy region:

1. The urban background station on Pascal Street in the city of Milan, characterized by a highly urbanized environment.
2. The urban traffic station on Senato Street in the city of Milan, also in an urban setting.
3. The rural background station in Schivenoglia, situated in the Mantua province in South Eastern Lombardy, known for its predominantly agricultural surroundings.

For the sake of simplicity, we will refer to these air quality stations as follows: the background station in Milan (Pascal), the traffic station in Milan (Senato), and the rural station in Schivenoglia. Notice that ammonium salt data are available for all stations until August 2020. However, for the rural station, data prior to February 2018 is not available. In Figure 1, the geographical locations of each air quality station within the

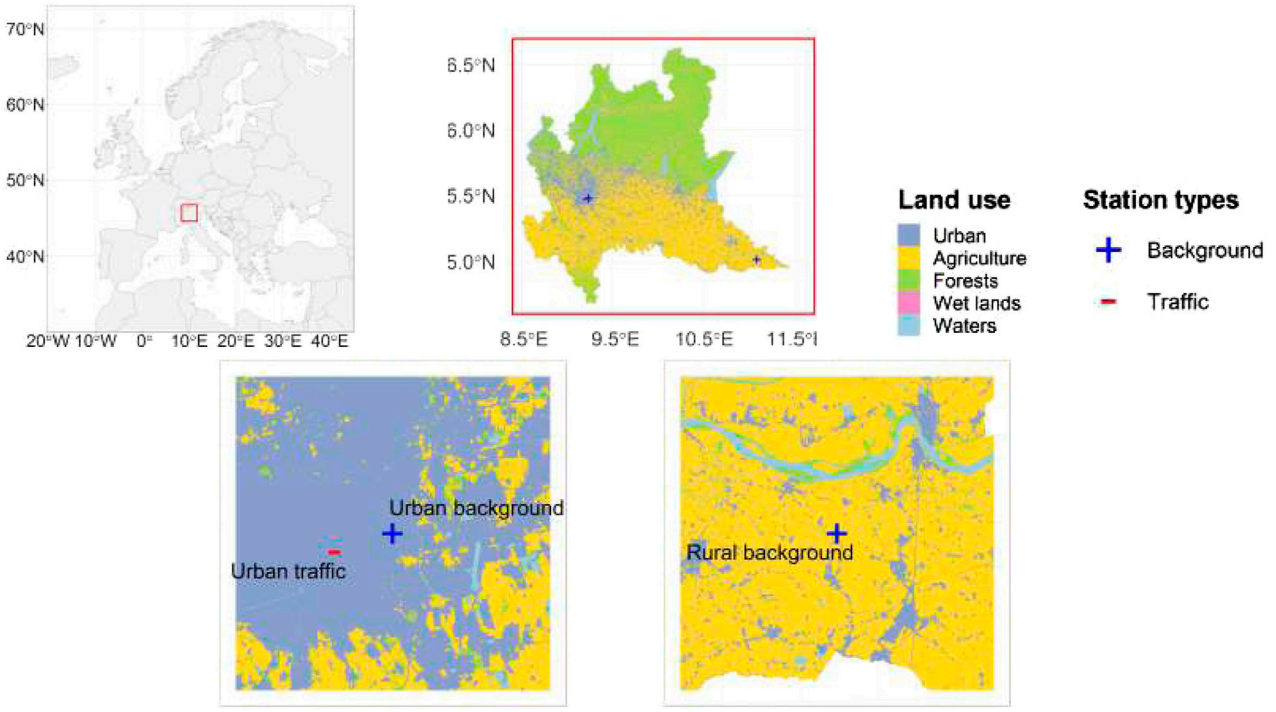

FIGURE 1
Air quality stations with respect to land use in Lombardy. Land use categories are urban areas, agricultural areas, forests, wetlands, and waters (colored in grey, yellow, green, violet, and light blue, respectively). The blue cross identifies background stations, while the red one identifies traffic stations. Map of Europe with a red rectangle over Lombardy.

region are displayed in relation to land use categories, which include urban areas (colored in grey), agricultural areas (yellow), forests (green), wetlands (violet), and bodies of water (light blue). Notice that livestock specialization prevails in the Lombardy plain to the east of Milan, which is much more limited in the west, where the prevalent specialized crop is rice paddy (Regione Lombardia, 2019).

Meteorological conditions, namely, wind speed and wind direction, have been sourced from weather station data available on the regional open data portal (Regione Lombardia, 2021). Since the meteorological and air quality stations are not co-located, we have associated weather conditions with air quality stations using the nearest weather station. Specifically, the nearest weather station for Milan's background air quality station (Juvara) is located approximately 1.2 kilometers (km) away. For Milan's traffic air quality station, the closest meteorological urban site (Brera) is situated approximately 660 m away. As for the rural air quality station, the nearest weather station is located in Sermide, a semi-urban environment in the province of Mantua, at a distance of 16 km. The lack of co-location between the monitoring stations may introduce minor measurement errors in attributing wind conditions. However, this is unlikely to significantly impact the analyses exploiting aggregate weather conditions under Section 3.2. In urban areas like Milan, small distances between stations do not typically result in major variations in wind speed and direction due to homogeneous meteorological conditions. For rural stations, such as those in the flat Manua province, distant weather stations likely still provide representative wind patterns, as topographical features have less influence on wind conditions.

Annual livestock consistencies are available on the data portal of the statistical office of the European Union (Eurostat) (Statistical Office of the European Union, 2023). Six-month data on livestock numbers are accessible through the National Data Bank of the Zootechnical Registry portal (Ministero della Salute, 2021). Regarding the spreading of livestock effluents (referred to as "spreading windows"), starting in 2016, the Regional Agency for Agricultural and Forestry Services (ERSAF) has been providing information twice a week through a bulletin that specifies permissible times for spreading within the six pedoclimatic zones in Lombardy: Alps, Western Prealps, Eastern Prealps, Western Plain, Central Plain, and Eastern Plain. We have obtained these data from the ERSAF website (Ente Regionale per i Servizi all'Agricoltura e alle Foreste, 2021). For a detailed overview of agricultural sources of ammonium salts, refer to Supplementary Section S4.

Information about land use and crop surfaces comes from a regional land use and cover database for the year 2018, known as *Destinazione d'Uso dei Suoli Agricoli e Forestali* (DUSAF), version 6.0 (Destination of use of agricultural and forest soils) (Regione Lombardia, 2019). Additionally, data on the regional and municipal borders for the year 2021 have been derived from the National Institute of Statistics (ISTAT) (Istituto Nazionale di Statistica, 2021). Lastly, annual population figures, observed all-cause mortality rates, and 3-year life expectancy data for the city of Milan were accessed through the Integrated Statistical System portal of the municipality (Comune di Milano, 2021).

2.2 Methods

2.2.1 Local wind patterns

Identifying sources of secondary pollutants that are not directly emitted into the atmosphere can be challenging. We employ a multifaceted approach that integrates various data sources and methods to accomplish this goal. In particular, we build upon the research conducted by Lonati and Cernuschi (2020), utilizing bivariate polar plot (BPP) and bivariate conditional probability distribution function (BCPF) analyses to investigate the relationship between daily concentrations of air pollutants and wind patterns. Notably, our analysis extends beyond NH_3, the focus of Lonati and Cernuschi (2020), to encompass PM_{10}, NH_4NO_3, and NO_x as well.

A BPP is a well-established technique for source apportionment. It represents concentration data using polar coordinates (reflecting wind direction) and radial coordinates (indicating a second numeric variable, typically wind speed). This approach provides insights into the probable distance and origin of sources that influence pollution levels at the receptor. We first partition the time series of atmospheric compound concentrations into bins based on wind speed and wind direction and then calculate averages. This method proves valuable in characterizing sources, facilitating the differentiation between diffuse, ground-level sources (such as livestock farms, residential heating, or traffic-related emissions) and point sources with buoyant emissions (including industrial plants, harbors, or airports), as demonstrated by Lonati and Cernuschi (2020). For further details, we refer to Carslaw et al. (2006), Carslaw and Ropkins (2012), Carslaw and Beevers (2013), Uria-Tellaetxe and Carslaw (2014), John H. Seinfeld (2016), and Grange and Carslaw (2019). We generate BPP and BCPF plots using the polarPlot function within the openair R package for air pollution analysis (Carslaw and Ropkins, 2012; Carslaw, 2019).

2.2.2 Long-range air mass patterns

We also employ long-range back-trajectory techniques to account for the potential influence of distant sources, given that SIA can persist in the atmosphere for up to 2 weeks and be transported. We use the HYbrid Single-Particle Lagrangian Integrated Trajectory (HYSPLIT) model version 5.3.2 (Stein et al., 2015) to derive 72-h air mass back-trajectories for our urban and rural background source receptors. For the simulation, trajectories are calculated daily at 00, 06, 12, and 18 universal Time Coordinated (UTC), starting from date 2013-01-01 to date 2020-08-01;at a height of 100 (Scotto et al., 2021) and 500;m (Ara Begum et al., 2005; Pekney et al., 2006; Zhao et al., 2007; Zhou et al., 2019; Scotto et al., 2021) above ground level (m a.g.l.), respectively. The HYSPLIT model, widely used for calculating atmospheric trajectories (Fleming et al., 2012), was developed by the National Oceanic and Atmospheric Administration (NOAA) Air Resources Laboratory. As meteorology data, we employ the National Center for Environmental Prediction (NCEP)/National Center for Atmospheric Research (NCAR) archived reanalysis data, with a 2.5° latitude-longitude resolution. We use the SplitR R package (Iannone, Richard, 2016) to apply the model and determine trajectories. As methods of analysis, we use the Potential Source Contribution Function (PSCF) and Concentration-Weighted Trajectory (CWT) methods, generated with the openair R package (Carslaw and Ropkins, 2012). The PSCF method provides spatially distributed conditional probabilities of highly polluting sources, based on a concentration percentile of interest (Ara Begum et al., 2005; Pekney et al., 2006; Zhao et al., 2007; Scotto et al., 2021). E.g., we apply PSCF to estimate likely sources contributing to concentrations above the 90th percentile. While PSCF relies on probabilities, the CWT method allows instead calculating a spatial weighted average of concentrations, providing complementary information on sources (Lupu and Maenhaut, 2002; Zhao et al., 2007; Masiol et al., 2015).

2.2.3 Health impacts from long-term concentration-response estimates

To evaluate the human health effects of agricultural activities that emit NH_3 and contribute to the formation of secondary inorganic aerosol (SIA) in a densely populated urban area as the city of Milan, we quantify the long-term health benefits of a hypothetical zero reduction of ammonium salts, a key inorganic component of PM_{10} associated with agriculture. Our study primarily examines the health effects in terms of attributable deaths (AD) and years of life lost (YLL) resulting from exposure to ammonium salts as a fraction of PM_{10} in Milan, using data from the urban background air quality station. We consider this station as representative of the broader study area. Despite ongoing but still insufficient research on the diverse toxicological properties of PM, we assume ammonium salts to possess comparable levels of toxicity to that of the total mass (Lim et al., 2012).

AD represent the number of individuals who have experienced premature mortality due to specific causes, such as exposure to air pollution, while YLL quantify the potential lifetime loss due to specific causes (European Environment Agency, 2022). To provide a comprehensive assessment, we compute AD and YLL for both the entire adult population of Milan aged 20 and older and for groups defined by year (y), gender (g), and age (a).

Deaths per year, gender, and age group $(D_{a,g,y})$ are attributed to air pollution using a population-attributable fraction $(1 - \frac{1}{RR_y})$ grounded in existing literature Eq. 1, obtaining attributable deaths $(AD_{a,g,y})$:

$$AD_{a,g,y} = D_{a,g,y} \times \left(1 - \frac{1}{RR_y}\right) \tag{1}$$

We exclude mortality from non-natural causes by applying a correction factor of 0.963 specific for the province of Milan taken from Carugno et al. (2017). The correction coefficient is constructed based on 2009–2013 mortality data and calculated excluding violent deaths.

The relative risk RR_y takes an exponential form:

$$RR_y = e^{(\beta \times (C_y - C_0))} \tag{2}$$

where C_y is the average annual SIA concentration and C_0 is the counterfactual level of no SIA pollution, thus C_0 is set to 0. Although some authors argue that under certain concentration levels PM has no effect on human health (Burnett and Cohen, 2020), this is far from being consensual (Papadogeorgou et al., 2019). In addition, given our exclusive focus on the SIA component, it would be reasonable to employ 0 as a threshold for a counterfactual scenario as it is highly improbable that SIA constitutes the

entirety of the annual PM mass (the median share in our data is around one-third).

In Eq. 2, β reflects the relative risk of long-term exposure to PM_{10} and is derived from Chen and Hoek (2020), who analyzed 17 cohort studies. The implied value of β is 0.003922 (CI: 0.002956–0.005827), meaning a 3.9% increase in the mortality rate for a 10 $\mu g/m^3$ increase in the long-term exposure to PM_{10}. Note that we apply the concentration-response functions to the adult subset of the population, which aligns with the prevailing cohorts across the studies considered by Chen and Hoek (2020). We obtain consistent results when applying the concentration-response functions to the general population.

The number of years of life lost per year, gender, and age group ($YLL_{a,g,y}$) is calculated by multiplying the expected remaining life years ($RLY_{a,g,y}$) by the number of deaths attributed to air pollution ($AD_{a,g,y}$):

$$YLL_{a,g,y} = RLY_{a,g,y} \times AD_{a,g,y} \tag{3}$$

Finally, we compute yearly aggregates Eqs. 4, 5 as well as the rates of attributable deaths and years of life lost per 100,000 inhabitants Eqs. 6, 7. This approach follows methodologies used in prior research (Carugno et al., 2017; Giannini et al., 2017).

$$AD_y = \sum_a \sum_g AD_{a,g,y} \tag{4}$$

$$YLL_y = \sum_a \sum_g YLL_{a,g,y} \tag{5}$$

$$ADR_y = \frac{\sum_y AD_y}{N_y} \times 100,000 \tag{6}$$

$$YLLR_y = \frac{\sum_y YLL_y}{N_y} \times 100,000 \tag{7}$$

where N_y is the total population in year y.

3 Results

3.1 Secondary inorganic aerosol's characterization

3.1.1 Summary statistics

Our data analysis begins with an overview of key pollutant concentrations observed at the three air quality stations, as summarized in Supplementary Tables S6–S8. Notably, PM_{10} levels across all stations are consistently high, and the average exceeds the proposed EU annual limit of 20 $\mu g/m^3$. From 2013 to 2020, PM_{10} at the urban background station frequently exceeds the proposed daily limit of 45 $\mu g/m^3$, on average 77 times a year, and has a mean concentration of 37 $\mu g/m^3$. Similarly, PM_{10} at the urban traffic station exceeds the proposed daily limit on average 66 times a year and has mean values of 36 $\mu g/m^3$. At the rural background site, exceedances are 47 a year, on average, and the mean concentration is 30 $\mu g/m^3$.

In winter, particulate levels between Milan and Schivenoglia are positively correlated. Specifically, NH_4NO_3 in the urban background station and PM_{10} in the rural station have a correlation of 0.77, while PM_{10} exhibits a correlation of 0.76, and NH_4NO_3 of 0.7. Moreover, NH_3 at the rural station shows a correlation of 0.33 with PM_{10} and 0.32 with NH_4NO_3 at the urban background (see the correlation matrices in Supplementary Figure S2).

TABLE 1 Percentiles of ammonium salts' share in PM_{10} for the urban background, traffic, and rural station (2013–2020).

	Percentile				
	0th	25th	50th	75th	100th
Background	0.03	0.17	0.25	0.36	0.94
Traffic	0.02	0.17	0.24	0.34	0.89
Rural	0.05	0.22	0.31	0.45	0.88

In the region, NO_x are mostly emitted by diesel engines (INEMAR - ARPA Lombardia, 2022) and their concentrations are substantially higher in urban areas than in rural areas (mean concentrations of 91, 100, and 25 $\mu g/m^3$ at the urban background station, urban traffic station, and the rural station, respectively). Conversely, 97% of NH_3 emissions come from agriculture; a gas that is found in greater concentrations in rural areas (mean of 20 $\mu g/m^3$) than in urban areas (9 $\mu g/m^3$ in the urban background).

3.1.2 Ammonium salts in PM

SIA is, on average, a third of PM_{10} (mean values of approximately 11 $\mu g/m^3$ for all three stations), and about three-fourths of SIA are NH_4NO_3. This is explained by the relative abundance of NO_x compared to SO_x in Lombardy and surrounding areas. A more detailed view of ammonium salts' shares in PM_{10} is given by Table 1 and Figure 2 on the percentile distribution, and by Supplementary Figure S3 on the time series of ammonium salts' share in PM_{10}. Ammonium salts are characterized by high temporal variability both within and between the monitoring stations, even within the same city. As expected, while $(NH_4)_2SO_4$ is constant throughout the year, NH_4NO_3 tends to peak in autumn and winter months, disappearing in the summer because of evaporation and decomposition at high temperatures (Lim et al., 2022), e.g., above 25° (Querol et al., 2016). Its sampling measure is further biased by volatilization from the filter (Chang et al., 2000; Schaap et al., 2002; Pirovano et al., 2015; Scotto et al., 2021). In all stations, the sole values of NH_4NO_3 often exceed the daily limit for PM_{10}. See Figure 3 that displays annualized mean concentration levels of PM_{10}, NH_4NO_3 and $(NH_4)_2SO_4$, respectively.

While there are no regulatory limits for NH_3 concentrations at the European level, ammonium salts significantly contribute to PM_{10} levels, often leading to exceedances of both the EU air quality limits and the internationally recommended values for health protection (Supplementary Tables S9–S11). The EU legislation currently allows a maximum of 35 days per year with PM_{10} concentrations above 50 $\mu g/m^3$, but discussions are considering revising these parameters, based on a European Commission legislative proposal that reduces the daily concentration threshold to 45 $\mu g/m^3$, and the maximum number of exceedances to 18 per year (European Commission, 2022). The WHO, however, recommends a PM_{10} limit of 45 $\mu g/m^3$, not to be exceeded more than 3–4 days yearly. Based on the 50 $\mu g/m^3$ EU limit, exceedances due to ammonium salts range from 0 to 16 days in Milan's background, 0 to 13 in traffic, and 1 to 6 in rural areas. The

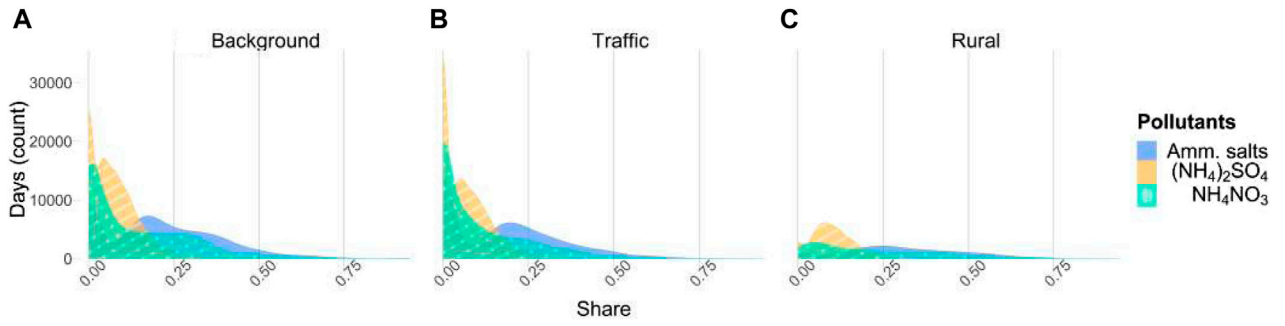

FIGURE 2
Frequency distribution plots of ammonium nitrates (NH_4NO_3), ammonium sulfates ($(NH_4)_2SO_4$), and ammonium salts daily shares (2013–2020) in PM_{10} concentrations (colored in green, yellow, and blue, respectively) at **(A)** the background, **(B)** traffic, and **(C)** rural air quality stations.

average overshoot above the 50 $\mu g/m^3$ threshold is 4.2, 3.5, and 4 in the urban background, urban traffic, and rural background, respectively. A more ambitious threshold of 45 $\mu g/m^3$ would increase these exceedances, with average overshoot values of 6.4, 5, and 5.7 at the respective stations. In 3 out of 8 years in Milan and 2 out of 3 years in the rural site, exceedances surpassed the 3–4 days limit set by WHO. For annual EU limits of PM_{10}, set at 40 $\mu g/m^3$ but potentially being revised to 20 $\mu g/m^3$, ammonium salts alone saturate around half of this limit. The average concentration is 11.6 $\mu g/m^3$ for the background and rural station, and 11.8 $\mu g/m^3$ for the traffic site. Considering the WHO recommended annual limit, ammonium salts constitute over 77% of the allowable PM_{10} in all stations.

3.2 The nexus between ammonium salts and agriculture

To investigate the temporal correlation of agriculture activities with the SIA levels measured in Milan, we calculate the cross-correlation between the NH_3 time series concentration levels registered in the rural areas near highly intensive livestock and NH_4NO_3 in the downwind Milan stations (Figure 4). The dashed horizontal lines represent the statistical significance of Pearson's cross-correlation coefficient. In Figure 4A, we observe a significant positive correlation between lagged NH_3 levels in the rural site and NH_4NO_3 levels in Milan's background, extending up to 2 days before. Similar findings are obtained when correlating NH_3 time series at the rural site with SIA at the traffic station, showing a positive correlation up to 2 days before NH_3 concentration increases are registered in heavily agriculture-dense regions (Figure 4B). This implies that fluctuations in agricultural activities emitting NH_3 are, on average, significantly correlated to the SIA concentrations observed in Milan up to 2 days after their occurrence. To verify that such cross-correlation is not due to weak dispersion with the build-up of all pollutants, we calculate the cross-correlation between NH_3 and the other pollutants as well. The cross-correlation with PM_{10} is not as straightforward as with NH_4NO_3: at the urban traffic station, it is positive and significant up to 1 day before, while at the urban background station only on the same day. This could be due to the PM_{10} composition variability, e.g., the relevance of primary sources compared to secondary ones, or the role of atmospheric conditions. Interestingly, lagged NH_3 is not significantly correlated with $(NH_4)_2SO_4$ at the urban site. This lack of correlation might indicate that NH_3 availability does not limit the sulfates levels or that other factors are more critical in determining their concentrations (e.g., sulfur dioxide emissions or meteorological conditions). For NO_x, the cross-correlation is positive on the same day but turns negative up to 5–7 days before. This inverse relationship suggests a complex dynamic, possibly indicating atmospheric chemistry interactions, where NH_3 presence could influence NO_x depletion over time. See Supplementary Figures S4–S6 for more details.

The formation of SIA depends not only on agricultural activities, as seen above but also on meteorological conditions and other pollutants. We analyze the seasonal polar plots of SIA and its precursors in Milan and the rural areas. Supplementary Figures S10–S12 show the average pollutant concentrations by wind conditions for each station and season. Strong seasonal patterns are observed for all stations, and a high variability characterizes each pollutant throughout the year. In particular, winter stands out as the season with the highest concentration values for PM_{10}, NH_4NO_3, and NO_x, when the frequent low inversion layer heights create the ideal conditions for pollution accumulation. With the exception of NH_3, high concentrations occur at low wind speeds below 3 meters per second (m/s). Moreover, PM_{10} and NH_4NO_3 share similar patterns as expected. Seasonal cycles appear analogous in both Milan's stations, though with wind pattern specificities. Interestingly, in Milan's background station (Supplementary Figure S10), NH_3 is most prevalent in autumn, when most of the spreading of effluents takes place (see Supplementary Figure S3 for a reference on spreading permits). Moreover, some of the highest levels are observed at medium wind speeds (2–3 m/s), while concentrations are lower when wind speed is below 2 m/s. This indicates that NH_3 is mostly transported into the city of Milan. NH_3 shows peculiar seasonal trends, likely stemming from its extended residence time of up to 10 days, enabling its transportation over long distances. Although we find evidence of NH_3 precursor being transported into Milan, the problem of SIA is clearly worsened by the specific meteorological conditions of the region, which favor pollution accumulation. NO_x, on the other hand, show trends of being mainly locally sourced in and around Milan. Unlike Milan, being relatively distant from large urban areas, the rural station is characterized by higher levels of NH_3, with a mean value one-fourth higher than the one recorded in the urban setting (Supplementary

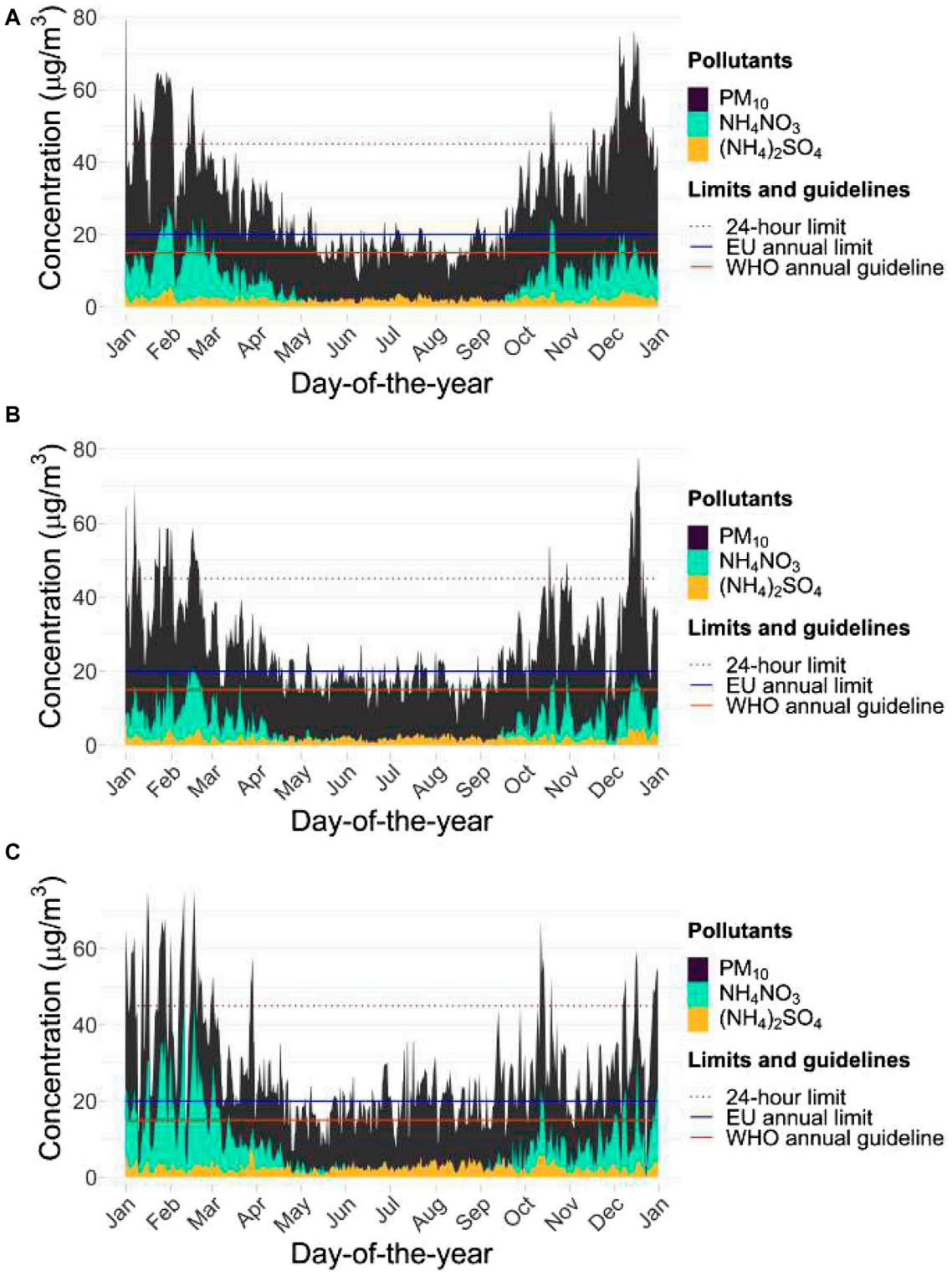

FIGURE 3
Time series of annualized daily mean concentration levels (2013–2020) for PM_{10}, NH_4NO_3, and $(NH_4)_2SO_4$ (colored in black, light green, and orange, respectively) at the following stations (stacked ammonium salts): **(A)** urban background, **(B)** urban traffic, and **(C)** rural background station. The daily and annual WHO guidelines for PM_{10} of 45 and 15 $\mu g/m^3$ are highlighted in red (with a dotted and a solid line, respectively). Over the period, the SIA mass in PM_{10} alone exceeded the daily limit 51, 40, and 17 times in the urban background, traffic, and rural station, respectively.

Figure S12). Moreover, summer is the predominant season for NH_3, with constant values around or above 20 $\mu g/m^3$, regardless of where the wind blows or at what speed. In fact, higher temperature and radiance induce gas-phase pollutants such as NH_3 to become more volatile (Abeed et al., 2022). NO_x behavior indicates that it is mainly transported from the east, where big cities are located.

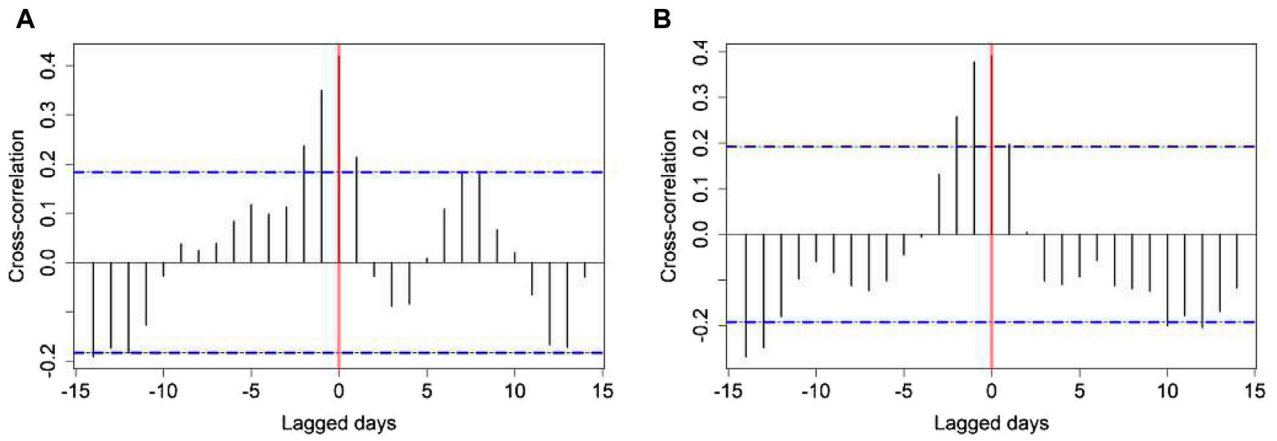

FIGURE 4
Pearson's cross-correlation plots between pollutants' time series in Milan air quality stations and Schivenoglia for winter months only (December, January, February). **(A)** Lagged NH_3 at the rural station and NH_4NO_3 at the background station. **(B)** Lagged NH_3 at the rural station and NNH_4NO_3 at the traffic station.

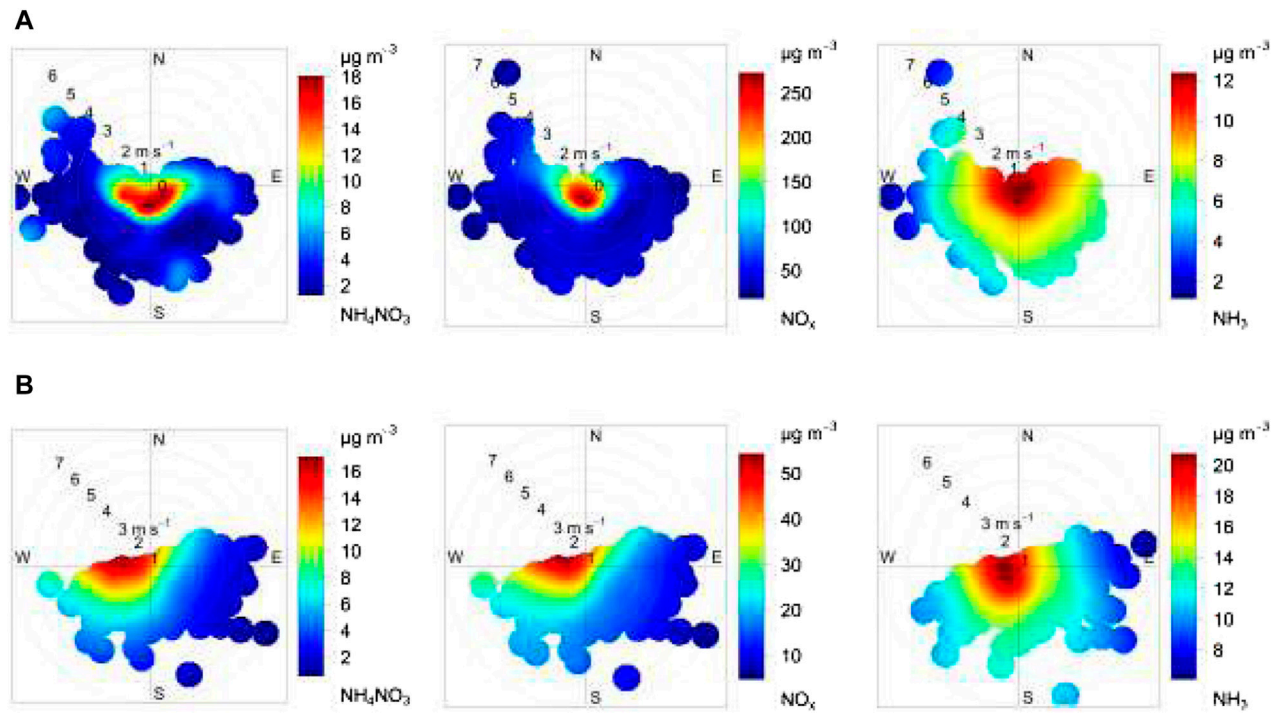

FIGURE 5
BPP for 2013–2020 mean levels of NH_4NO_3, NO_x, and NH_3 in $\mu g/m^3$ at the **(A)** Milan background and **(B)** rural station.

To derive insights from specific concentration ranges, we exploit the BCPF technique developed by Uria-Tellaetxe and Carslaw (2014), which puts together the conditional probability function approach with that of polar plots. This way, the BCPF plot associates a probability to a specific concentration level bin, eventually identifying potential sources. We first focus on the worse case pollution episodes and compare the BCPF plots for the range of concentrations > 90th percentile (Supplementary Figures S13–15). Lombardy's most critical SIA pollution episodes happen with very low winds, favorable to accumulation when pollution builds up in the atmosphere for several days. This trend is observed for all the stations. In the Milanese background, NH_4NO_3 and NO_x peak concentrations occur when the winds blow from the south-southwest and southeast at very low wind speeds, around or less than 1 m/s (Supplementary Figure S13). The southeast, northeast, and east-northeast regions, characterized by a high density of cattle and swine (see also Supplementary Table S8), show the greatest likelihood of NH_3 concentrations. The BPP confirms that homogeneously scattered sources surround the receptor location (Figure 5A). Unlike the Milan

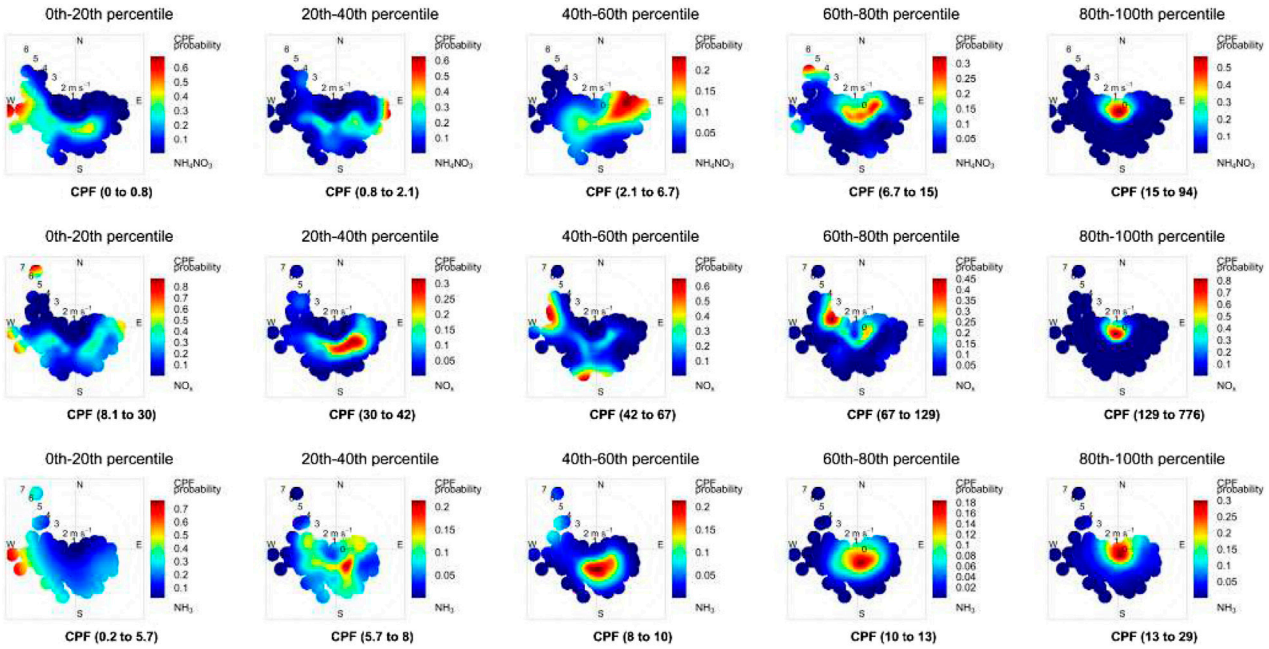

FIGURE 6
BCPF bins for NH_4NO_3, NO_x, and NH_3 at Milan's background station. Concentration ranges in $\mu g/m^3$ are in round brackets.

background station, at the traffic area station, the northern quadrants have the greatest impact on pollution episodes (Supplementary Figures S14, 16). Conversely, the western quadrants appear to prevail in affecting pollution at the rural receptor (Figures 5B, Supplementary Figure S15).

Based on recent relevant literature, air pollution sources may be associated with specific concentration ranges (Uria-Tellaetxe and Carslaw, 2014). After having focused on concentration peaks, we use BCPF to find evidence of transported *versus* locally produced SIA and its precursors. In addition, we examine the average concentrations of pollutants below and above specific threshold values to investigate the wind conditions linked to recommended and undesirable air quality levels. In Figures 6–8, we show BCPF plots for NH_4NO_3 concentrations every 20 percentiles between the 0th and the 100th percentile (e.g., between the 0th and the 20th percentile). On the one hand, while average polar plots provide a general picture of the influence of wind, they are not satisfactory for identifying sources. On the other hand, in the context of the Po Valley, focusing only on the highest percentiles may limit attention to accumulation episodes. Binned polar plots highlight the multitude of sources and their spatial variability as a function of concentration ranges. The graphs show how the various sources scattered around the monitoring sites interact with the meteorological conditions and contribute differently to SIA levels. In Milan's background (Figure 6), we observe that the lower concentration ranges are typically linked to moderate to high wind speeds, originating from the west, south-west, and south-east (0th-20th and 20th-40th percentile), which can quickly transport NH_4NO_3 from afar to the city. For concentrations between the 40th and the 60th percentile, we find once again evidence of transportation from the east and southwest at medium wind speeds (2–4 m/s). Overall, the plot shows how concentrations are often transported to the city, the exception being the extreme pollution episodes at higher concentrations, between 15 and 94 $\mu g/m^3$, when the low wind speed effect plays a major role in the accumulation of pollution. In Milan's background, NH_4NO_3 values above 5 $\mu g/m^3$ seem to be associated with lower wind speeds, while values below 5 $\mu g/m^3$ confirm NO_x locally (Supplementary Figure S17). Figure 7 shows clear transport phenomena occurring at the traffic station, except for the upper percentiles, associated with accumulation conditions. Supplementary Figure S18 confirms the transport of ammonium salts towards the traffic receptor, in particular for concentrations below 5 $\mu g/m^3$. The limited amount of values of NO_x below 10 $\mu g/m^3$ does not allow plotting the BPP for the traffic station. Regarding the rural background, the high SIA concentration episodes happen at the intersection of NO_x and NH_3 concentrated air. While, there is no evidence of frequent locally formed SIA episodes, as the NO_x concentrations in this rural region are lower, and NO_x are likely to be the limiting precursor (Figure 8). Regarding threshold plots for rural areas, the higher concentrations of SIA, NO_x, and NH_3 are linked to sources located in the west-northwest (Supplementary Figure S19). Moreover, NO_x appear to be mostly transported. Importantly, in Milan, NO_x are locally sourced, contrary to what happens in the rural site. NH_3, on the other hand, is mostly transported into the city.

Finally, we generate plots of ratios between the cumulative mass of ammonium salts and the total mass of PM_{10} (Supplementary Figure S20). This visualization helps us identify weather conditions where the inorganic component contributes significantly to PM. In the first panel, which pertains to Milan's background station, it is evident that for nearby localized sources and when winds originate from the east, ammonium salts play a more significant role than for other wind conditions. This trend also extends to cases with strong winds from the west-southwest. Therefore, PM_{10} coming from the east, where the majority of livestock units are located (see Supplementary Figures S7–9), consistently contains a higher proportion of SIA. Similarly, in the second panel on the traffic station, transport patterns are detectable

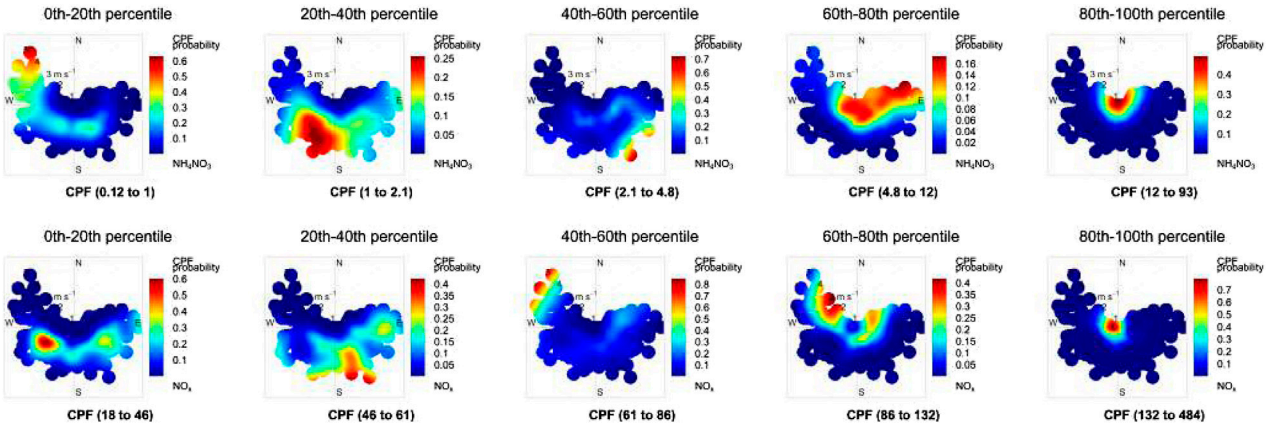

FIGURE 7
BCPF bins for NH_4NO_3 and NO_x at Milan traffic station. Concentration ranges in $\mu g/m^3$ are in round brackets.

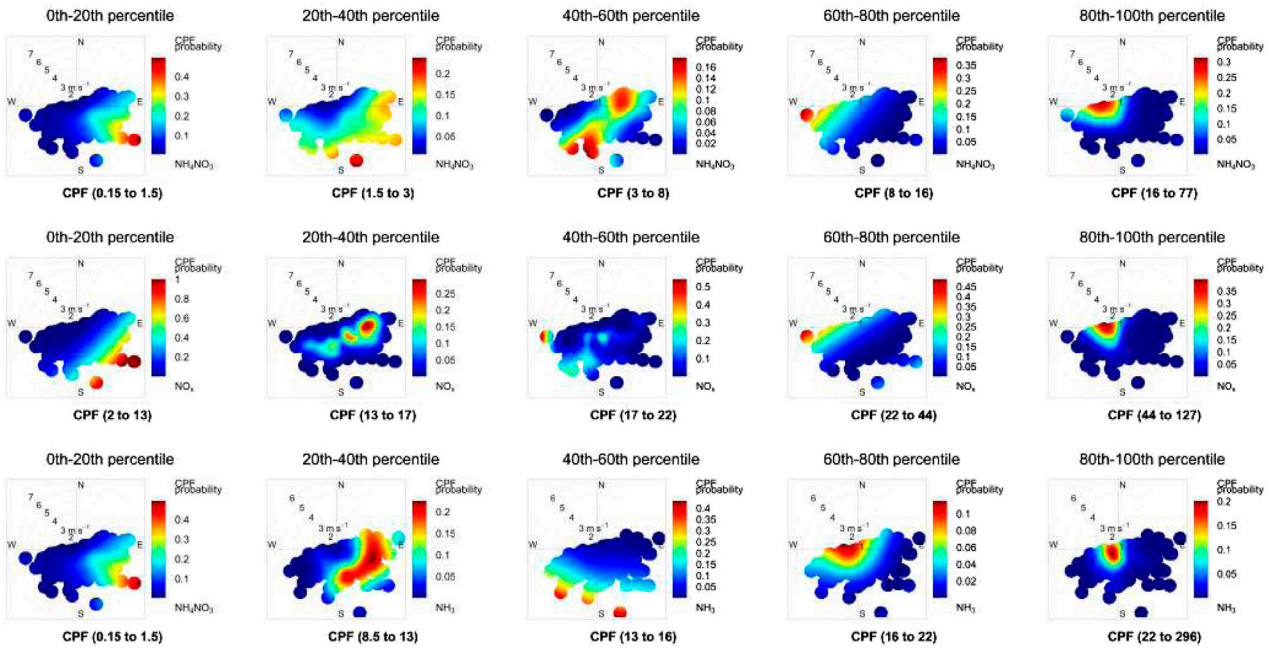

FIGURE 8
BCPF bins for NH_4NO_3, NO_x, and NH_3 at Schivenoglia station. Concentration ranges in $\mu g/m^3$ are in round brackets.

with northeast and east winds and in the case of sources close to the monitoring site. Conversely, in the rural areas, the ratio with the total mass increases when westerly and southwest winds prevail. In such instances, the higher SIA in PM_{10} composition is linked to NO_x sources located west of the receptor (third panel). All in all, we find evidence that the NO_x sources in the city of Milan interact with NH_3, primarily transported from the rural sites, resulting in the formation of SIA and in the increase of already hazardous levels of PM_{10}.

Concerning Milan's SIA levels, various graphical analyses have suggested a significant impact from regions known for high livestock density. One of the agricultural activities with a substantial impact on SIA formation is the broadcasting of livestock manure (Pohl et al., 2022; Wyer et al., 2022). We look at the correlation between this activity and the observed SIA levels in Milan, analyzing what happened before and after a spreading event in the Western Plain to which Milan belongs. Figures 9A,B show NH_4NO_3 concentration levels at the background site for cold months between October and February *versus* the days before and after a spreading event (±5 days) in Lombardy (2016–2020). It is evident that the median value of NH_4NO_3 is lower prior to a spreading event, in contrast to the day of the event and the subsequent 3 days. This result holds not only for the median but also for the daily average. Relative to the day prior to the broadcasting, the level of NH_4NO_3 rises by 2 $\mu g/m^3$ on the spreading day and reaches its maximum on the subsequent day with an increase of 3 $\mu g/m^3$ before tapering off in the days that follow. Note that these graphs merely serve as suggestive evidence, as they

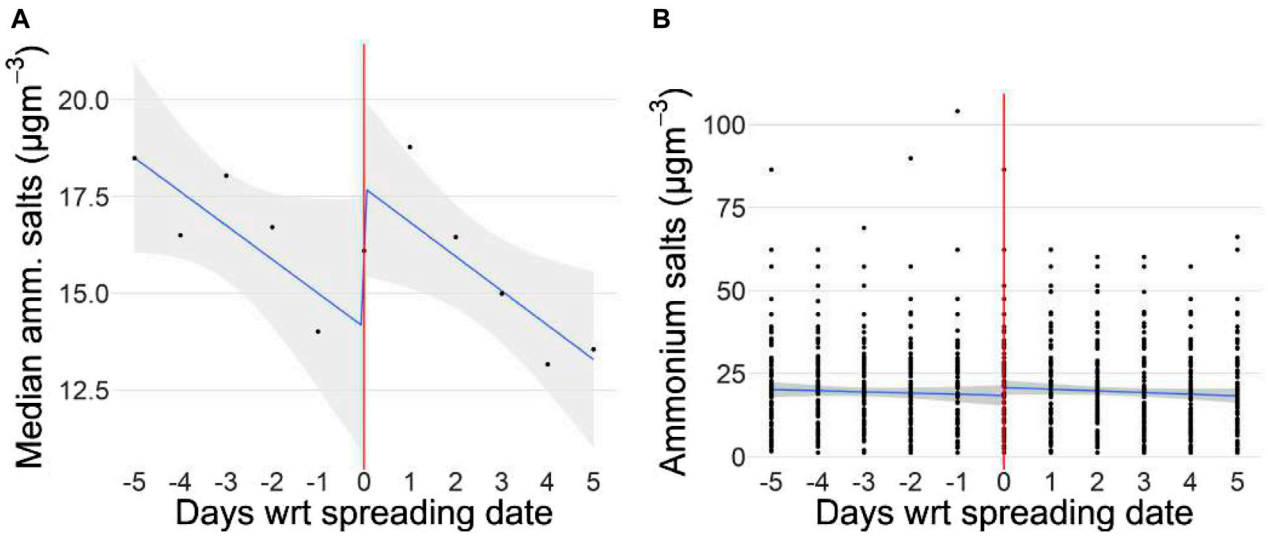

FIGURE 9
Scatter plots of ammonium salt levels in $\mu g/m^3$ at the background station for cold months only (October to February) and days close to a spreading event (±5) in Lombardy (2016–2020): **(A)** Median ammonium salts and **(B)** daily ammonium salts. A fitted line is colored in blue, with grey CI.

do not include any other variables. To determine causality, further investigation into the relationship between spreading and ammonium salt levels is needed. We repeat the analysis for the traffic station, obtaining similar results (Supplementary Figure S21).

After having looked at local contributions to air pollution, we turn to long-range contributions. Back-trajectory techniques have been applied in the Po Valley context in relation to different pollutants and time spans (Sogacheva et al., 2007; Hamed et al., 2007; Masiol et al., 2012; Diémoz et al., 2019; Scotto et al., 2021). We derive 3-day back-trajectories at the urban background receptor location in Milan at 500;m a.g.l. between 01 January 2013 and 29 February 2020, at 0:00, 6:00, 12:00, and 18:00 UTC, excluding months when COVID-19 restrictions were put in place across Europe (Eurostat, 2022).

In Supplementary Figures S22–S24, we show the Potential Source Contribution Function (PSCF) and the Concentration Weighted Trajectory (CWT) seasonal plots for NH_4NO_3 derived for different heights. The PSCF displays the probability that sources of concentrations >90th percentile at the receptor are located in a certain grid cell. The PSCF plot highlights the influence of long-range transboundary pollution towards the receptor site from across most continental Europe and the Mediterranean and across all seasons. However, it does not allow differentiating between relevant sources (Stojić and Stanišić Stojić, 2017). The CWT plot shows the relative importance of emission sources by taking into account concentration gradients over trajectories. In winter, multiple locations appear relevant for the highest concentrations, such as the Hammamet Gulf in Tunisia, the Aragon and Catalonia regions in Spain, the Turkish Marmara region, the Algerian coastal area, and the Adriatic coast. In autumn, both sources from the Mediterranean and continental Europe are evident. Such areas may be linked to point sources, such as industrial areas, harbors, and airports. However, when focusing on specific concentration ranges local influences emerge. E.g., constraining to concentrations below the 75th percentile (12 $\mu g/m^3$) or between the first and third quartile (1–12 $\mu g/m^3$), local sources around Northern Italy stand out in winter (see Figures 10 and Supplementary Figure S25). See Supplementary Figure S26 on concentrations <99th percentile (47.9 $\mu g/m^3$) as well. Also looking at concentrations above the 90th (21.8 $\mu g/m^3$) and 99th percentile, local sources play a role (see Supplementary Figures S27, 28).

3.3 Health impacts attributable to exposure to ammonium salts in Milan

As a final stage, we shift our focus to evaluating the impact of agriculture-related inorganic PM_{10} on human health. We employ health impact functions from prior epidemiological research, applying them exclusively to ammonium salts to achieve this. For the purpose of this study, we consider all PM_{10} particles to pose an equal level of toxicity to human health as the total PM_{10} mass (Lim et al., 2012). Table 2 shows the annual number of deaths (AD) and years of life lost (YLL) and related rates for every 100,000 inhabitants (ADR and YLLR) in the city of Milan between 2013 and 2019 attributable to exposure to ammonium salts above 0 $\mu g/m^3$. Notice that we exclude 2020 due to data distortions caused by the COVID-19 pandemic (Granella et al., 2021). In Milan, an average of 589 people per year lost their lives due to ammonium salts between 2013 and 2019, resulting in a mean count of 6,951 YLL. In terms of premature deaths per 100,000 inhabitants, the figures varied from a minimum of 37 in 2014 to a maximum of 54 in 2017, averaging 43. The total years lost per 100,000 due to ammonium salts ranged from 439 to 648, with an average of 511. In summary, over the 7-year period, 4,123 people experienced premature mortality, resulting in a total loss of 48,659 years of life. It is worth noting that the health impacts trend remained stationary in the period considered. In Tables 3 and 4, we present the average attributable deaths and

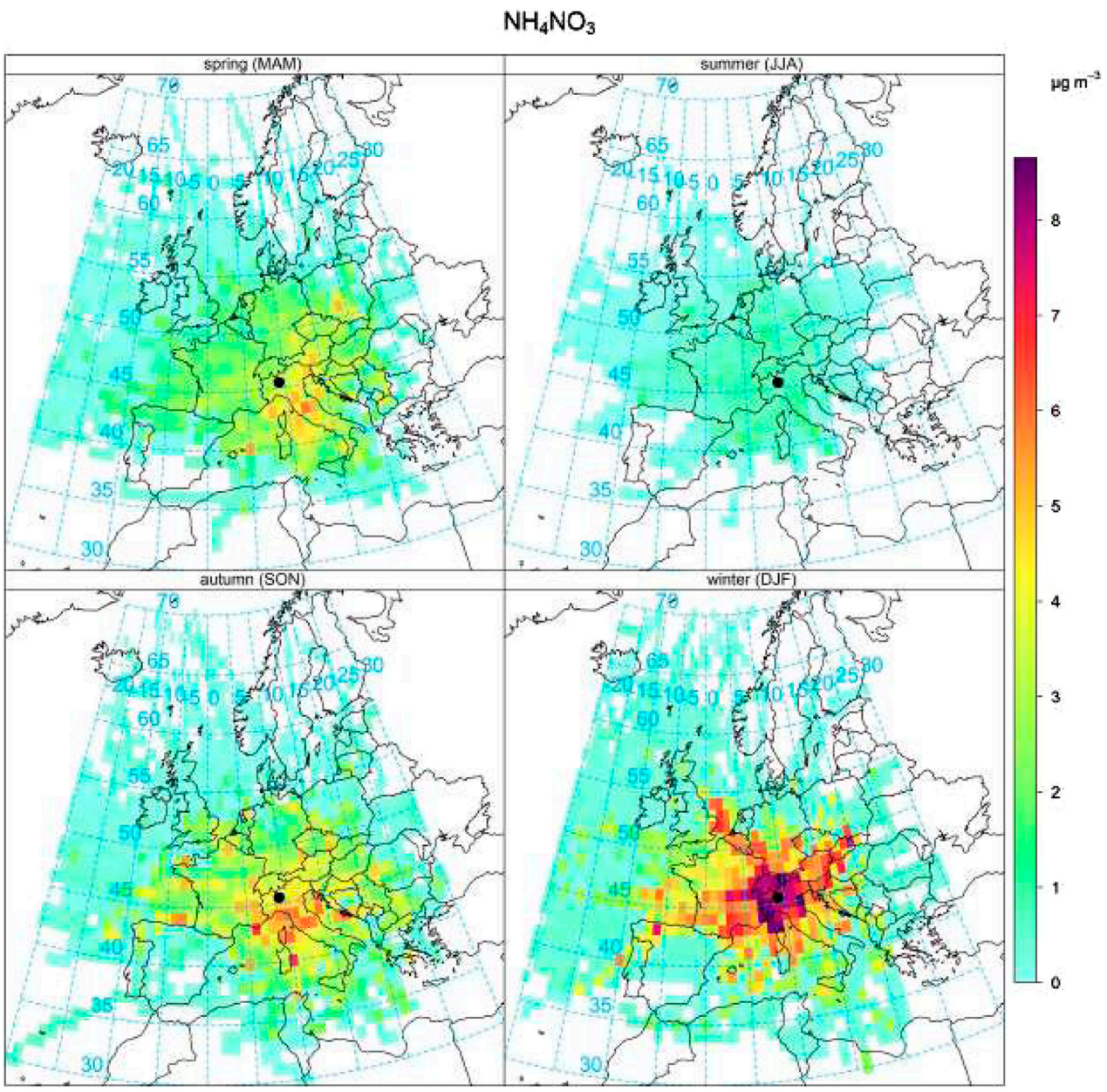

FIGURE 10
Seasonal gridded 72-h back-trajectory NH_4NO_3 concentrations derived from the Concentration Weighted Trajectory (CWT) approach applied on concentrations <75th percentile at the urban background source receptor in Milan at 500;m a.g.l. between 01 January 2013 and 29 February 2020, at 0: 00, 6:00, 12:00, and 18:00 UTC. The CWT cell values are the concentration weighted means. The location of the source receptor is identified with a black dot.

years of life lost by gender and quinquennial age group for the period 2013–2019. As expected, deaths attributed to inorganic pollution vary across age groups, generally rising with increasing age. Moreover, these deaths tend to be more prevalent among males, except for women aged 85 and above, who bear the highest mortality burden. Although limited, deaths associated with inorganic pollution are also estimated among the younger generations, likely impacting the youth population's most vulnerable and fragile segments. To our knowledge, the existing literature does not provide a specific beta value for long-term exposure to PM_{10} tailored to the Milanese context or associated with a comparable average exposure within a similar cohort context. To account for the uncertainty in our estimates, we recalculated the health impacts using the 95% CI for the relative risk used to derive the β, ranging from 1.03 to 1.06 (Supplementary Tables S15–S18). The lower bound estimated attributable deaths (AD) are 446, resulting in 5,267 YLL, which equates to 33 AD and 387 YLL per 100,000 population. In the upper bound scenario, there were 866 attributable deaths, resulting in 10,222 years of life lost, with rates of 64 attributable deaths and 751 years of life lost per 100,000 population.

TABLE 2 Annual attributable deaths (AD), years of life lost (YLL), attributable deaths rate (ADR), and years of life lost rate (YLLR) every 100,000 inhabitants in Milan (2013–2019) due to long-term exposure to ammonium salts as a fraction of PM_{10} above 0 $\mu g/m^3$ measured at Pascal background station (β of 0.003922 from pooled RR of 1.04).

Year	2013	2014	2015	2016	2017	2018	2019
AD	575	489	586	566	740	598	569
YLL	7019	5867	6827	6798	8852	6854	6442
ADR	43	37	44	42	54	43	40
YLLR	530	439	507	503	648	491	458

4 Discussion

In the region of Lombardy, located in Northern Italy, the agricultural sector stands as the primary source of ammonia (NH_3) emissions, a key precursor to secondary inorganic aerosol (SIA) (INEMAR - ARPA Lombardia, 2022). Building on a study by Lonati and Cernuschi (2020), our work proposes a characterization of the contribution of the agricultural sector to PM_{10} pollution in Lombardy by analyzing concentrations of its inorganic component, i.e., ammonium nitrate (NH_4NO_3) and ammonium sulfate ($(NH_4)_2SO_4$), also jointly known as ammonium salts. We examine the conditions under which emissions deriving from agriculture contribute to high PM_{10} concentrations and, consequently, to an increase in negative health outcomes for its population. Our work informs local and regional policymakers on the characterization of the SIA formation in Lombardy and provides insights to support effective mitigation policy decisions.

We find that, at the air quality stations analyzed and especially in rural areas, SIA accounts for a significant portion of the overall PM_{10} mass, often exceeding 30%. NH_4NO_3 dominates the composition of SIA, highlighting the importance of long-term regional air pollution control measures aimed at reducing NH_4NO_3 and its gaseous precursors, NH_3 and nitrogen oxides (NO_x).

In winter, pollution levels between cities are positively correlated, implying similar trends regardless of local sources, while SIA in Milan's background air quality station correlates less to NH_3 in the rural areas of Schivenoglia, suggesting that aerosol may have reacted during transit, showing signs of transport. NH_3 in the rural context significantly correlates with SIA in Milan on the same day and with lags, up to 2 days. In Milan, there is evidence of transport of NH_3, particularly from the eastern quadrants, where intensive livestock activities are highly concentrated, while NO_x seem to be mainly localized. In rural areas, high concentrations of NH_3 and NO_x mostly come from the west, and the highest levels of SIA are recorded when the wind blows from areas where NO_x are concentrated. Local sources also stand out in back-trajectory modeling of concentrations.

We also find suggestive evidence of the relationship between manure spreading and SIA. Our observations indicate a 2 micrograms per cubic meter of air ($\mu g/m^3$) increase in SIA levels at the urban background station on the day of manure spreading in neighboring areas, followed by an additional 3 $\mu g/m^3$ increase on a subsequent day. While there are no regulatory limits for NH_3 concentrations at the European level, ammonium salts contribute considerably to breaching PM_{10} limit values. Ammonium salts saturate around half of the currently under discussion EU annual limit of 20 $\mu g/m^3$ with values between 11.6 and 11.8 $\mu g/m^3$ at the air quality stations considered, while the plausible daily limit of 45 $\mu g/m^3$ is exceeded on average 6.4, 5, and 5.7 times. This confirms the relevant role of agriculture in exacerbating poor air quality, overshooting EU limits and WHO-recommended standards for health protection, and causing adverse health effects.

Annually, 589 [446–866] deaths and 6,951 [5,267–10,222] years of life, equivalent to 43 [33–64] and 511 [387–751] every 100,000 inhabitants, are lost on average in Milan due to pollution linked to agricultural activities that could be curbed with technological abatement measures without reducing production. Although referring to $PM_{2.5}$ and not to the inorganic component of PM_{10}, findings drawn from the Global Burden of Disease data and from EEA's analyses exhibit similar magnitudes. In Italy, exposure to ambient $PM_{2.5}$ was linked to an estimated 24,700 premature deaths and approximately 356,000 years of life lost, equivalent to 41 attributable deaths (CI: 32–50) and 591 years of life lost (CI: 476–713) per 100,000 population (Insitute for Health Metrics and

TABLE 3 2013–2019 mean attributable deaths (AD) by quinquennial age and gender in Milan due to long-term exposure to ammonium salts as a fraction of PM_{10} above 0 $\mu g/m^3$ measured at Pascal background station (β of 0.003922 from pooled RR of 1.04).

	Mean AD											
	30–34	35–39	40–44	45–49	50–54	55–59	60–64	65–69	70–74	75–79	80–84	≥ 85
Females	0.6	1.1	1.9	3.5	5.4	6.6	8.8	13.6	20	32	49.8	164.6
Males	1.3	1.6	2.9	4.6	7.8	10.6	14.3	20.6	29.1	42.9	52.1	93.3

TABLE 4 2013–2019 mean years of life lost (YLL) by quinquennial age and gender in Milan due to long-term exposure to ammonium salts as a fraction of PM_{10} above 0 $\mu g/m^3$ measured at Pascal background station (β of 0.003922 from pooled RR of 1.04).

	Mean YLL											
	30–34	35–39	40–44	45–49	50–54	55–59	60–64	65–69	70–74	75–79	80–84	≥ 85
Females	35	54.3	82.3	138.4	189.7	199.0	226.6	289.8	342.9	420.5	476.3	1080.4
Males	66.6	70.4	118.6	164.6	242.8	279.6	315.8	370.8	415.7	465	407.8	498.5

Evaluation, 2019). According to the EEA, the nationwide premature deaths for exposure to $PM_{2.5}$ above 5 $\mu g/m^3$ are 46,800, resulting in 415,400 YLL, equivalent to 88 AD and 701 YLL per 100,000 population (European Environment Agency, 2023b). More specifically, if measures had been taken to reduce $PM_{2.5}$ levels in the metropolitan city of Milan, 124 deaths per 100,000 residents could have been avoided, as well as 1,182 lost years could have been saved (European Environment Agency, 2023a). Therefore, rates of health impacts attributable to exposure to ammonium salts concentrations exceeding 0 $\mu g/m^3$, assuming similar toxicity to PM_{10}, are relevant and comparable to the nationwide rates of impacts of $PM_{2.5}$ concentrations exceeding 5 $\mu g/m^3$. Single-sector policies alone will not yield substantial reductions in SIA. Rather, a multifaceted approach that simultaneously addresses emissions from traffic, thermal plants, and agricultural activities (especially livestock effluent management) is required to achieve substantial reductions.

We acknowledge several limitations to our study. The estimation method of ammonium salts is based on the assumption that salts are pure, though this may not be the case, biasing our estimates. We apply long-term concentration-response functions to determine the number of nonaccidental deaths attributable to exposure to ammonium salts, even though on the one hand they were originally constructed for the PM_{10} total mass and on the other hand not specifically for the city of Milan. We also assume ammonium salts to have comparable levels of toxicity to that of the total mass, while the literature on the differential toxicity of PM remains limited and with mixed results. Finally, despite the presence of missing values in the data, it is worth noting that the length of our time series mitigates this concern.

Our research adds to an expanding body of literature that explores the impact of agriculture on air quality, specifically focusing on their association rather than causality. However, investigating the causal effect in future studies would be of great interest. Our study also provides insights into the health consequences of secondary air pollution in an urban environment heavily influenced by agricultural activities. Furthermore, our research highlights the importance of PM speciation data and underscores the value of making this information accessible to the public for research purposes and for raising awareness of the complexity of PM pollution.

Data availability statement

The datasets presented in this study can be found in online repositories. The names of the repository/repositories and accession number(s) can be found below: 10.17632/2mzdnzfwmt.1.

Author contributions

SR: Conceptualization, Data curation, Formal Analysis, Investigation, Methodology, Software, Visualization, Writing–original draft, Writing–review and editing. JL: Conceptualization, Investigation, Writing–review and editing, Methodology. FG: Investigation, Writing–review and editing, Data curation. MM: Conceptualization, Investigation, Writing–review and editing, Methodology. DD: Investigation, Resources, Supervision, Writing–review and editing, Data curation.

Funding

The author(s) declare that financial support was received for the research, authorship, and/or publication of this article. This research has received funding from the Fondazione CARIPLO under the project “INHALE—Impact on human Health of Agriculture and Livestock Emissions,” and from the "GRINS-Growing Resilient, INclusive and Sustainable" project (GRINS PE00000018).

Acknowledgments

We thank ARPA Lombardia for providing the PM_{10} speciation data, for their support on ammonium salts calculation, and for their useful comments and suggestions. We also thank participants at the AgriAir, AGRIMONIA, and INHALE conferences for fruitful discussions. We acknowledge and thank the CMCC Foundation—Euro-Mediterranean Center on Climate Change and the RFF-CMCC European Institute on Economics and the Environment (RFF-CMCC EIEE) for granting the infrastructure and services to perform this work. We gratefully acknowledge the NOAA Air Resources Laboratory (ARL) for the provision of the HYSPLIT transport and dispersion model and the NCEP/NCAR reanalysis data used in this publication. SR is grateful to Lara Aleluia Reis from RFF-CMCC EIEE for her continued support and professional input, to Federica Nobile from the Department of Epidemiology of the Lazio Region (Italy), and to Saurabh Annadate from the Department of Pure and Applied Sciences of the University of Urbino “Carlo Bo” (Italy) for their helpful comments.

Conflict of interest

The authors declare that the research was conducted in the absence of any commercial or financial relationships that could be construed as a potential conflict of interest.

Publisher’s note

Supplementary material

The Supplementary Material for this article can be found online at: https://www.frontiersin.org/articles/10.3389/fenvs.2024.1369678/full#supplementary-material

References

Abeed, R., Viatte, C., Porter, W. C., Evangeliou, N., Clerbaux, C., Clarisse, L., et al. (2022). Estimating agricultural ammonia volatilization over Europe using satellite observations and simulation data. *EGUsphere. [preprint]*. doi:10.5194/egusphere-2022-1046

Achilleos, S., Kioumourtzoglou, M.-A., Wu, C.-Da, Schwartz, J. D., Koutrakis, P., and Papatheodorou, S. I. (2017). Acute effects of fine particulate matter constituents on mortality: a systematic review and meta-regression analysis. *Environ. Int.* 109, 89–100. doi:10.1016/j.envint.2017.09.010

Aksoyoglu, S., Ciarelli, G., El-Haddad, I., Baltensperger, U., and Prévôt, A. S. H. (2017). Secondary inorganic aerosols in Europe: sources and the significant influence of biogenic VOC emissions, especially on ammonium nitrate. *Atmos. Chem. Phys.* 17 (12), 7757–7773. ISSN 1680-7324. doi:10.5194/acp-17-7757-2017

Amato, F., van Drooge, B. L., Jaffrezo, J. L., Favez, O., Colombi, C., Cuccia, E., et al. (2024). Aerosol source apportionment uncertainty linked to the choice of input chemical components. *Environ. Int.* 184, 108441. ISSN 0160-4120. doi:10.1016/j.envint.2024.108441

Andreani-Aksoyoglu, S., Prévôt, A. S. H., Baltensperger, U., Keller, J., and Dommen, J. (2004). Modeling of formation and distribution of secondary aerosols in the Milan area (Italy). *J. Geophys. Res. Atmos.* 109 (D5). ISSN 0148-0227. doi:10.1029/2003jd004231

Ara Begum, B., Kim, E., Jeong, C.-H., Lee, D.-W., and Hopke, P. K. (2005). Evaluation of the potential source contribution function using the 2002 Quebec forest fire episode. *Atmos. Environ.* 39 (20), 3719–3724. ISSN 1352-2310. doi:10.1016/j.atmosenv.2005.03.008

Atkinson, R. W., Mills, I. C., Walton, H. A., and Ross Anderson, H. (2014). Fine particle components and health—a systematic review and meta-analysis of epidemiological time series studies of daily mortality and hospital admissions. *J. Expo. Sci. Environ. Epidemiol.* 25 (2), 208–214. doi:10.1038/jes.2014.63

Badaloni, C., Cesaroni, G., Cerza, F., Davoli, M., Brunekreef, B., and Forastiere, F. (2017). Effects of long-term exposure to particulate matter and metal components on mortality in the Rome longitudinal study. *Environ. Int.* 109, 146–154. doi:10.1016/j.envint.2017.09.005

Baek, B. H., Aneja, V. P., and Tong, Q. (2004). Chemical coupling between ammonia, acid gases, and fine particles. *Environ. Pollut.* 129 (1), 89–98. doi:10.1016/j.envpol.2003.09.022

Bedogni, M., and Pirovano, G. (2011). Source apportionment technique: inorganic aerosol transformation processes in the Milan area. *Int. J. Environ. Pollut.* 47 (1/2/3/4), 167. ISSN 1741-5101. doi:10.1504/ijep.2011.047333

Belis, C. A., Pirovano, G., Villani, M. G., Calori, G., Pepe, N., and Putaud, J. P. (2021). Comparison of source apportionment approaches and analysis of non-linearity in a real case model application. *Geosci. Model. Dev.* 14 (7), 4731–4750. doi:10.5194/gmd-14-4731-2021

Burnett, R., and Cohen, A. (2020). Relative risk functions for estimating excess mortality attributable to outdoor PM2.5 air pollution: evolution and state-of-the-art. *Atmosphere* 11, 589. doi:10.3390/atmos11060589

Cambra-López, M., Aarnink, A. J. A., Zhao, Y., Calvet, S., and Torres, A. G. (2010). Airborne particulate matter from livestock production systems: a review of an air pollution problem. *Environ. Pollut.* 158 (1), 1–17. doi:10.1016/j.envpol.2009.07.011

Carozzi, M., Ferrara, R., Fumagalli, M., Sanna, M., Chiodini, M., Perego, A., et al. (2012). Field-scale ammonia emissions from surface spreading of dairy slurry in Po Valley. *Italian J. Agrometorology* 17, 25–34.

Carslaw, D., Beevers, S., Ropkins, K., and Bell, M. (2006). Detecting and quantifying aircraft and other on-airport contributions to ambient nitrogen oxides in the vicinity of a large international airport. *Atmos. Environ.* 40 (28), 5424–5434. doi:10.1016/j.atmosenv.2006.04.062

Carslaw, D. C. (2019). The openair manual — open-source tools for analysing air pollution data. *Man. version* 2, 6. Available at: https://davidcarslaw.com/files/openairmanual.pdf.

Carslaw, D. C., and Beevers, S. D. (2013). Characterising and understanding emission sources using bivariate polar plots and k-means clustering. *Environ. Model. Softw.* 40, 325–329. doi:10.1016/j.envsoft.2012.09.005

Carslaw, D. C., and Ropkins, K. (2012). Openair — an R package for air quality data analysis. *Environ. Model. Softw.* 27-28, 52–61. doi:10.1016/j.envsoft.2011.09.008

Caserini, S., Giani, P., Cacciamani, C., Ozgen, S., and Lonati, G. (2017). Influence of climate change on the frequency of daytime temperature inversions and stagnation events in the Po Valley: historical trend and future projections. *Atmos. Res.* 184, 15–23. doi:10.1016/j.atmosres.2016.09.018

Cassee, F. R., Héroux, M.-E., Gerlofs-Nijland, M. E., and Kelly, F. J. (2013). Particulate matter beyond mass: recent health evidence on the role of fractions, chemical constituents and sources of emission. *Inhal. Toxicol.* 25 (14), 802–812. doi:10.3109/08958378.2013.850127

Chang, M. C., Sioutas, C., Kim, S., Gong, H., and Linn, W. S. (2000). Reduction of nitrate losses from filter and impactor samplers by means of concentration enrichment. *Atmos. Environ.* 34 (1), 85–98. ISSN 1352-2310. doi:10.1016/s1352-2310(99)00308-8

Chen, J., and Hoek, G. (2020). Long-term exposure to PM and all-cause and cause-specific mortality: a systematic review and meta-analysis. *Environ. Int.* 143, 105974. doi:10.1016/j.envint.2020.105974

Chen, S., Zhao, Y., and Zhang, R. (2018). Formation mechanism of atmospheric ammonium bisulfate: hydrogen-bond-promoted nearly barrierless reactions of SO_3 with NH_3 and H_2O. *ChemPhysChem* 19 (8), 967–972. doi:10.1002/cphc.201701333

Chiara Pietrogrande, M., Biffi, B., Colombi, C., Cuccia, E., Dal Santo, U., and Romanato, L. (2024). Contribution of chemical composition to oxidative potential of atmospheric particles at a rural and an urban site in the Po Valley: influence of high ammonia agriculture emissions. *Atmos. Environ.* 318, 120203. ISSN 1352-2310. doi:10.1016/j.atmosenv.2023.120203

Chung, Y., Dominici, F., Wang, Y., Coull, B. A., and Bell, M. L. (2015). Associations between long-term exposure to chemical constituents of fine particulate matter ($PM_{2.5}$) and mortality in medicare enrollees in the eastern United States. *Environ. Health Perspect.* 123 (5), 467–474. doi:10.1289/ehp.1307549

Clappier, A., Thunis, P., Beekmann, M., Putaud, J. P., and de Meij, A. (2021). Impact of SOx, NOx and NH3 emission reductions on PM2.5 concentrations across Europe: hints for future measure development. *Environ. Int.* 156, 106699. doi:10.1016/j.envint.2021.106699

Colombo, L., Marongiu, A., Fossati, G., Malvestiti, G., and Angelino, E. (2024). Pm2.5 wintertime sensitivity to changes in nox, so2, and nh3 emissions in Lombardy region. *Air Qual. Atmos. Health*. ISSN 1873-9326. doi:10.1007/s11869-024-01519-0

Comune di Milano (2021). *Sistema statistico integrato*. Available at: http://sisi.comune.milano.it/.

Daher, N., Ruprecht, A., Invernizzi, G., Marco, C.De, Miller-Schulze, J., Bae Heo, J., et al. (2012). Characterization, sources and redox activity of fine and coarse particulate matter in Milan, Italy. *Atmos. Environ.* 49, 130–141. ISSN 1352-2310. doi:10.1016/j.atmosenv.2011.12.011

Diémoz, H., Barnaba, F., Magri, T., Pession, G., Dionisi, D., Pittavino, S., et al. (2019). Transport of Po valley aerosol pollution to the northwestern Alps – Part 1: phenomenology. *Atmos. Chem. Phys.* 19 (5), 3065–3095. ISSN 1680-7324. doi:10.5194/acp-19-3065-2019

Ehrnsperger, L., and Klemm, O. (2021). Source apportionment of urban ammonia and its contribution to secondary particle formation in a mid-size European city. *Aerosol Air Qual. Res.* 21 (5), 200404. doi:10.4209/aaqr.2020.07.0404

Ente Regionale per i Servizi all'Agricoltura e alle Foreste (2021). *Bollettino nitrati*. Available at: https://www.ersaf.lombardia.it/it/servizi-al-territorio/nitrati/bollettini-nitrati/archivio-bollettino-nitrati.

European Commission (2022). *Proposal for a Directive of the European Parliament and of the Council on ambient air quality and cleaner air for Europe*. Available at: https://eur-lex.europa.eu/legal-content/EN/TXT/?uri=CELEX:52022PC0542 (Accessed October 26, 2023).

European Environment Agency (2022). Air quality in Europe 2022. *Tech. Rep.*

European Environment Agency (2023a). European environment and health atlas. Available at: https://discomap.eea.europa.eu/atlas/.

European Environment Agency (2023b). Harm to human health from air pollution in Europe: burden of disease 2023. *Tech. Rep.*

European Environment Agency (2023c). National air pollutant emissions data viewer 2005-2021. Available at: https://www.eea.europa.eu/data-and-maps/dashboards/necd-directive-data-viewer-7.

European Union (2008). Directive 2008/50/EC of the European Parliament and of the Council of 21 May 2008 on ambient air quality and cleaner air for Europe. *Tech. Rep.*

Eurostat (2022). Impact of Covid-19 crisis on industrial production. Available at: https://ec.europa.eu/eurostat/.

Fassò, A., Rodeschini, J., Fusta Moro, A., Shaboviq, Q., Maranzano, P., Cameletti, M., et al. (2023). Agrimonia: a dataset on livestock, meteorology and air quality in the Lombardy region, Italy. *Sci. Data* 10 (1), 143. ISSN 2052-4463. doi:10.1038/s41597-023-02034-0

Fleming, Z. L., Monks, P. S., and Review, A. J. M. (2012). Review: untangling the influence of air-mass history in interpreting observed atmospheric composition. *Atmos. Res.* 104–105, 1–39. ISSN 0169-8095. doi:10.1016/j.atmosres.2011.09.009

Fu, J., Fei, F., Wang, S., Qi, Z., Yang, X., Zhong, J., et al. (2023). Short-term effects of fine particulate matter constituents on mortality considering the mortality displacement in Zhejiang province, China. *J. Hazard. Mater.* 457, 131723. doi:10.1016/j.jhazmat.2023.131723

Giannadaki, D., Elias, G., Pozzer, A., and Lelieveld, J. (2018). Estimating health and economic benefits of reductions in air pollution from agriculture. *Sci. Total Environ.* 622-623, 1304–1316. doi:10.1016/j.scitotenv.2017.12.064

Giannini, S., Baccini, M., Randi, G., Bonafè, G., Lauriola, P., and Ranzi, A. (2017). Estimating deaths attributable to airborne particles: sensitivity of the results to different exposure assessment approaches. *Environ. Health* 16 (1), 13. doi:10.1186/s12940-017-0213-9

Granella, F., Reis, L. A., Bosetti, V., and Tavoni, M. (2021). Covid-19 lockdown only partially alleviates health impacts of air pollution in northern Italy. *Environ. Res. Lett.* 16 (3), 035012. ISSN 1748-9326. doi:10.1088/1748-9326/abd3d2

Granella, F., Renna, S., and Reis, L. A. (2024). The formation of secondary inorganic aerosols: a data-driven investigation of Lombardy's secondary inorganic aerosol problem. *Atmos. Environ.* 327, 120480. ISSN 1352-2310. doi:10.1016/j.atmosenv.2024.120480

Grange, S. K., and Carslaw, D. C. (2019). Using meteorological normalisation to detect interventions in air quality time series. *Sci. Total Environ.* 653, 578–588. doi:10.1016/j.scitotenv.2018.10.344

Hamed, A., Joutsensaari, J., Mikkonen, S., Sogacheva, L., Dal Maso, M., Kulmala, M., et al. (2007). Nucleation and growth of new particles in Po Valley, Italy. *Atmos. Chem. Phys.* 7 (2), 355–376. ISSN 1680-7324. doi:10.5194/acp-7-355-2007

Iannone, Richard (2016). *splitr*. Available at: https://github.com/rich-iannone/SplitR.

INEMAR - ARPA Lombardia (2022). *INEMAR, Inventario Emissioni in Atmosfera: emissioni in Regione Lombardia nell'anno 2019 - versione in revisione pubblica*. Milan, Italy: ARPA Lombardia Settore Monitoraggi Ambientali. Available at: https://www.inemar.eu (Accessed: July 22, 2023).

Insitute for Health Metrics and Evaluation (2019). Global burden of disease. Available at: https://vizhub.healthdata.org/gbd-results/.

Istituto Nazionale di Statistica (2021). *Istituto Nazionale di Statistica*. Available at: https://www.istat.it/it/archivio/222527.

Kinney, P. L., Roman, H. A., Walker, K. D., Richmond, H. M., Conner, L., and Hubbell, B. J. (2010). On the use of expert judgment to characterize uncertainties in the health benefits of regulatory controls of particulate matter. *Environ. Sci. Policy* 13 (5), 434–443. doi:10.1016/j.envsci.2010.05.002

Larsen, B. R., Gilardoni, S., Stenström, K., Niedzialek, J., Jimenez, J., and Belis, C. A. (2012). Sources for PM air pollution in the Po Plain, Italy: II. Probabilistic uncertainty characterization and sensitivity analysis of secondary and primary sources. *Atmos. Environ.* 50, 203–213. doi:10.1016/j.atmosenv.2011.12.038

Lee, C. J., Martin, R. V., Henze, D. K., Brauer, M., Cohen, A., and van Donkelaar, A. (2015). Response of global particulate-matter-related mortality to changes in local precursor emissions. *Environ. Sci. Technol.* 49 (7), 4335–4344. ISSN 1520-5851. doi:10.1021/acs.est.5b00873

Lelieveld, J., Evans, J. S., Fnais, M., Giannadaki, D., and Pozzer, A. (2015). The contribution of outdoor air pollution sources to premature mortality on a global scale. *Nature* 525 (7569), 367–371. doi:10.1038/nature15371

Lim, J. H., Park, H. Y., and Cho, S. Y. (2022). Evaluation of the ammonia emission sensitivity of secondary inorganic aerosol concentrations measured by the national reference method. *Atmos. Environ.* 270, 118903. doi:10.1016/j.atmosenv.2021.118903

Lim, S. S., Vos, T., Flaxman, A. D., Danaei, G., Shibuya, K., Adair-Rohani, H., et al. (2012). A comparative risk assessment of burden of disease and injury attributable to 67 risk factors and risk factor clusters in 21 regions, 1990–2010: a systematic analysis for the Global Burden of Disease Study 2010. *Lancet* 380 (9859), 2224–2260. doi:10.1016/s0140-6736(12)61766-8

Lonati, G., and Cernuschi, S. (2020). Temporal and spatial variability of atmospheric ammonia in the Lombardy region (Northern Italy). *Atmos. Pollut. Res.* 11 (12), 2154–2163. doi:10.1016/j.apr.2020.06.004

Lonati, G., Giugliano, M., and Ozgen, S. (2008). Primary and secondary components of PM2.5 in Milan (Italy). *Environ. Int.* 34 (5), 665–670. ISSN 0160-4120. doi:10.1016/j.envint.2007.12.009

Lovarelli, D., Conti, C., Finzi, A., Bacenetti, J., and Guarino, M. (2020). Describing the trend of ammonia, particulate matter and nitrogen oxides: the role of livestock activities in northern Italy during Covid-19 quarantine. *Environ. Res.* 191, 110048. doi:10.1016/j.envres.2020.110048

Lovarelli, D., Fugazza, D., Costantini, M., Conti, C., Diolaiuti, G., and Guarino, M. (2021). Comparison of ammonia air concentration before and during the spread of COVID-19 in Lombardy (Italy) using ground-based and satellite data. *Atmos. Environ.* 259, 118534. doi:10.1016/j.atmosenv.2021.118534

Lunghi, J., Malpede, M., and Reis, L. A. (2024). Exploring the impact of livestock on air quality: a deep dive into ammonia and particulate matter in Lombardy. *Environ. Impact Assess. Rev.* 105, 107456. ISSN 0195-9255. doi:10.1016/j.eiar.2024.107456

Lupu, A., and Maenhaut, W. (2002). Application and comparison of two statistical trajectory techniques for identification of source regions of atmospheric aerosol species. *Atmos. Environ.* 36 (36–37), 5607–5618. ISSN 1352-2310. doi:10.1016/s1352-2310(02)00697-0

Masiol, M., Benetello, F., Harrison, R. M., Formenton, G., De Gaspari, F., and Spatial, B. P. (2015). Spatial, seasonal trends and transboundary transport of PM2.5 inorganic ions in the Veneto region (Northeastern Italy). *Atmos. Environ.* 117, 19–31. ISSN 1352-2310. doi:10.1016/j.atmosenv.2015.06.044

Masiol, M., Squizzato, S., Ceccato, D., Rampazzo, G., and Bruno, P. (2012). Determining the influence of different atmospheric circulation patterns on PM10 chemical composition in a source apportionment study. *Atmos. Environ.* 63, 117–124. ISSN 1352-2310. doi:10.1016/j.atmosenv.2012.09.025

McDuffie, E. E., Martin, R. V., Spadaro, J. V., Burnett, R., Smith, S. J., O'Rourke, P., et al. (2021). Source sector and fuel contributions to ambient PM2.5 and attributable mortality across multiple spatial scales. *Nat. Commun.* 12 (1), 3594. doi:10.1038/s41467-021-23853-y

Metrohm AG. 930 compact ic flex - manual (2017). *Metrohm AG. 930 compact ic flex - manual*. Available at: https://www.metrohm.com/it_it/products/2/9301/29301100.html (Accessed February 22, 2024).

Michele, C., Consonni, D., Pier, A. B., Biggeri, A., and Baccini, M. (2017). Temporal trends of PM10 and its impact on mortality in Lombardy, Italy. *Environ. Pollut.* 227, 280–286. doi:10.1016/j.envpol.2017.04.077

Ministero della Salute (2021). *Banca dati Nazionale dell'Anagrafe zootecnica*. Available at: https://www.vetinfo.it/j6_statistiche/#/.

Otto, P., Fusta Moro, A., Rodeschini, J., Shaboviq, Q., Ignaccolo, R., Golini, N., et al. (2024). Spatiotemporal modelling of PM2.5 concentrations in Lombardy (Italy): a comparative study. *Environ. Ecol. Statistics* 31, 245–272. ISSN 1573-3009. doi:10.1007/s10651-023-00589-0

Papadogeorgou, G., Kioumourtzoglou, M.-A., Braun, D., and Zanobetti, A. (2019). Low levels of air pollution and health: effect estimates, methodological challenges, and future directions. *Curr. Environ. Health Rep.* 6 (3), 105–115. doi:10.1007/s40572-019-00235-7

Park, M., Hung, S. J., Lee, K., Jang, M., Kim, S. D., Kim, I., et al. (2018). Differential toxicities of fine particulate matters from various sources. *Sci. Rep.* 8 (1), 17007. ISSN 2045-2322. doi:10.1038/s41598-018-35398-0

Pekney, N. J., Davidson, C. I., Zhou, L., and Hopke, P. K. (2006). Application of PSCF and CPF to PMF-Modeled Sources of PM2.5 in Pittsburgh. *Aerosol Sci. Technol.* 40 (10), 952–961. ISSN 1521-7388. doi:10.1080/02786820500543324

Perrone, M. G., Zhou, J., Malandrino, M., Sangiorgi, G., Rizzi, C., Ferrero, L., et al. (2016). PM chemical composition and oxidative potential of the soluble fraction of particles at two sites in the urban area of Milan, Northern Italy. *Atmos. Environ.* 128, 104–113. ISSN 1352-2310. doi:10.1016/j.atmosenv.2015.12.040

Pietrogrande, M. C., Demaria, G., Colombi, C., Cuccia, E., and Santo, U. D. (2022). Seasonal and Spatial Variations of PM10 and PM2.5 Oxidative Potential in Five Urban and Rural Sites across Lombardia Region, Italy. *Int. J. Environ. Res. Public Health* 19 (13), 7778. ISSN 1660-4601. doi:10.3390/ijerph19137778

Pirovano, G., Colombi, C., Balzarini, A., Riva, G. M., Gianelle, V., and Lonati, G. (2015). PM2.5 source apportionment in Lombardy (Italy): comparison of receptor and chemistry-transport modelling results. *Atmos. Environ.* 106, 56–70. doi:10.1016/j.atmosenv.2015.01.073

Pohl, V., Gilmer, A., Hellebust, S., McGovern, E., Cassidy, J., Byers, V., et al. (2022). Ammonia cycling and emerging secondary aerosols from arable agriculture: a European and Irish perspective. *Air* 1 (1), 37–54. doi:10.3390/air1010003

Pozzer, A., Tsimpidi, A. P., Karydis, V. A., de Meij, A., and Lelieveld, J. (2017). Impact of agricultural emission reductions on fine-particulate matter and public health. *Atmos. Chem. Phys.* 17 (20), 12813–12826. ISSN 1680-7324. doi:10.5194/acp-17-12813-2017

Pretolani, R., and Rama, D. (2022). "Il sistema agro-alimentare della Lombardia," in *Rapporto 2022*. Milan, Italy: Franco Angeli.

Querol, X., Karanasiou, A., Amato, F., Vasconcelos, C., Alastuey, A., Viana, M., et al. (2016). AIRUSE - testing and development of air quality mitigation measures in Southern Europe. PM speciation and source apportionment. Available at: https://airuse.eu/.

Regione Lombardia (2018). *Dusaf 6.0 - uso del suolo*. Available at: https://www.dati.lombardia.it/Territorio/Dusaf-6-0-Uso-del-suolo-2018/7rae-fng6.

Regione Lombardia (2019). *Uso e copertura del suolo 2018 (DUSAF 6.0)*. Available at: https://www.geoportale.regione.lombardia.it/en/.

Regione Lombardia (2021). *Open data lombardia*. Available at: https://dati.lombardia.it/.

Schaap, M., Müller, K., and ten Brink, H. M. (2002). Constructing the European aerosol nitrate concentration field from quality analysed data. *Atmos. Environ.* 36 (8), 1323–1335. doi:10.1016/s1352-2310(01)00556-8

Schlesinger, R. B., and Cassee, F. (2003). Atmospheric secondary inorganic particulate matter: the toxicological perspective as a basis for health effects risk assessment. *Inhal. Toxicol.* 15 (3), 197–235. doi:10.1080/08958370304503

Scotto, F., Bacco, D., Lasagni, S., Trentini, A., Poluzzi, V., and Vecchi, R. (2021). A multi-year source apportionment of PM2.5 at multiple sites in the southern Po Valley (Italy). *Atmos. Pollut. Res.* 12 (11), 101192. ISSN 1309-1042. doi:10.1016/j.apr.2021.101192

Seinfeld, J. H., and Pandis, S. N. (2016). *Atmospheric chemistry and physics: from air pollution to climate Change*. Hoboken, NJ: John Wiley and Sons Inc. Available at: https://www.ebook.de/de/product/25599491/john_h_seinfeld_spyros_n_pandis_atmospheric_chemistry_and_physics_from_air_pollution_to_climate_change.html.

Sogacheva, L., Hamed, A., Facchini, M. C., Kulmala, M., and Laaksonen, A. (2007). Relation of air mass history to nucleation events in Po Valley, Italy, using back trajectories analysis. *Atmos. Chem. Phys.* 7 (3), 839–853. ISSN 1680-7324. doi:10.5194/acp-7-839-2007

Squizzato, S., Masiol, M., Brunelli, A., Pistollato, S., Tarabotti, E., Rampazzo, G., et al. (2013). Factors determining the formation of secondary inorganic aerosol: a case study in the Po Valley (Italy). *Atmos. Chem. Phys.* 13 (4), 1927–1939. doi:10.5194/acp-13-1927-2013

Statistical Office of the European Union (2023). Animal populations by NUTS 2 regions. Available at: https://ec.europa.eu/eurostat/.

Stein, A. F., Draxler, R. R., Rolph, G. D., Stunder, B. J. B., Cohen, M. D., and Ngan, F. (2015). NOAA's HYSPLIT atmospheric transport and dispersion modeling System. *Bull. Am. Meteorological Soc.* 96 (12), 2059–2077. ISSN 1520-0477. doi:10.1175/bams-d-14-00110.1

Stojić, A., and Stanišić Stojić, S. (2017). The innovative concept of three-dimensional hybrid receptor modeling. *Atmos. Environ.* 164, 216–223. ISSN 1352-2310. doi:10.1016/j.atmosenv.2017.06.009

Teledyne API (2019). *The model T201 chemiluminescence NH analyzer*. Available at: https://www.teledyne-api.com/(Accessed February 22, 2024).

Thakrar, S. K., Balasubramanian, S., Adams, P. J., Azevedo, I. M. L., Muller, N. Z., Pandis, S. N., et al. (2020). Reducing mortality from air pollution in the United States by targeting specific emission sources. *Environ. Sci. Technol. Lett.* 7 (9), 639–645. doi:10.1021/acs.estlett.0c00424

Thermo Fisher Scientific Inc (2021). *Thermo scientific model 17i - ammonia chemiluminescent gas analyzer*. Available at: https://www.thermofisher.com/ (Accessed February 22, 2024).

Thunis, P., Clappier, A., Beekmann, M., Philippe Putaud, J., Cuvelier, C., Madrazo, J., et al. (2021). Non-linear response of $PM_{2.5}$ to changes in NO_x and NH_3 emissions in the Po basin (Italy): consequences for air quality plans. doi:10.5194/acp-2021-65

Tuomisto, J. T., Wilson, A., Evans, J. S., and Tainio, M. (2008). Uncertainty in mortality response to airborne fine particulate matter: combining European air pollution experts. *Reliab. Eng. Syst. Saf.* 93 (5), 732–744. doi:10.1016/j.ress.2007.03.002

UNI EN 12341:2023 (2023). *Aria ambiente - Metodo gravimetrico di riferimento per la determinazione della concentrazione in massa di particolato sospeso PM10 o PM2,5*. Technical report.

UNI EN 14211:2005 (2005). *Qualità dell'aria ambiente - Metodo normalizzato per la misurazione della concentrazione di diossido di azoto e monossido di azoto mediante chemiluminescenza*. Technical report.

UNI EN 14792:2017 (2017). *Emissioni da sorgente fissa - Determinazione della concentrazione massica di ossidi di azoto - Metodo di riferimento normalizzato: chemiluminescenza*. Technical report.

UNI EN 16913 (2017). Aria ambiente - Metodo di riferimento per la determinazione di NO, SO_2, Cl^-, NH, Na, K, Mg_2, Ca_2 contenuti nel PM2,5 depositati su filtri. *Tech. Rep.* 2017.

Uria-Tellaetxe, I., and Carslaw, D. C. (2014). Conditional bivariate probability function for source identification. *Environ. Model. Softw.* 59, 1–9. doi:10.1016/j.envsoft.2014.05.002

Van Damme, M., Clarisse, L., Whitburn, S., Hadji-Lazaro, J., Hurtmans, D., Clerbaux, C., et al. (2018). Industrial and agricultural ammonia point sources exposed. *Nature* 564 (7734), 99–103. doi:10.1038/s41586-018-0747-1

Van Damme, M., Wichink Kruit, R. J., Schaap, M., Clarisse, L., Clerbaux, C., Coheur, P.-F., et al. (2014). Evaluating 4 years of atmospheric ammonia (NH_3) over Europe using IASI satellite observations and LOTOS-EUROS model results. *J. Geophys. Res. Atmos.* 119 (15), 9549–9566. doi:10.1002/2014jd021911

Veratti, G., Stortini, M., Amorati, R., Bressan, L., Giovannini, G., Bande, S., et al. (2023). Impact of NOx and NH3 emission reduction on particulate matter across Po valley: a LIFE-IP-PREPAIR study. *Atmosphere* 14 (5), 762. doi:10.3390/atmos14050762

World Health Organization Regional Office for Europe (2013). *Review of evidence on health aspects of air pollution: REVIHAAP project: technical report*. Copenhagen, Denmark: World Health Organization. Available at: https://apps.who.int/iris/handle/10665/341712.

Wyer, K. E., Kelleghan, D. B., Blanes-Vidal, V., Schauberger, G., and Curran, T. P. (2022). Ammonia emissions from agriculture and their contribution to fine particulate matter: a review of implications for human health. *J. Environ. Manag.* 323, 116285. doi:10.1016/j.jenvman.2022.116285

Wyzga, R. E., and Rohr, A. C. (2015). Long-term particulate matter exposure: attributing health effects to individual PM components. *J. Air and Waste Manag. Assoc.* 65 (5), 523–543. ISSN 2162-2906. doi:10.1080/10962247.2015.1020396

Zhao, W., Hopke, P. K., and Zhou, L. (2007). Spatial distribution of source locations for particulate nitrate and sulfate in the upper-midwestern United States. *Atmos. Environ.* 41 (9), 1831–1847. ISSN 1352-2310. doi:10.1016/j.atmosenv.2006.10.060

Zhou, C., Zhou, H., Holsen, T. M., Hopke, P. K., Edgerton, E. S., and Schwab, J. J. (2019). Ambient ammonia concentrations across New York State. *J. Geophys. Res. Atmos.* 124 (14), 8287–8302. ISSN 2169-8996. doi:10.1029/2019jd030380